

# Removal of Nutrients from Water Using Biosurfactant Micellar Enhanced Ultrafiltration

Sarjana Binte Rafiq Era

A thesis  
In the Department of  
Building, Civil, and Environmental Engineering

Presented in Partial Fulfillment of the Requirements  
For the Degree of  
Master of Applied Science (Civil Engineering)

Concordia University  
Montreal, Quebec, Canada

August 2022

©Sarjana Binte Rafiq Era, 2022

CONCORDIA UNIVERSITY  
SCHOOL OF GRADUATE STUDIES

This is to certify that the thesis is prepared

By: Sarjana Binte Rafiq Era

Entitled: Removal of nutrients from water using Micellar Enhanced Ultrafiltration using biosurfactant

and submitted in partial fulfillment of the requirements for the degree of

Master of Applied Science (Civil Engineering)

complies with the regulations of the University and meets the accepted standards concerning originality and quality.

Signed by the final examining committee:

\_\_\_\_\_ Chair

Dr. Ashutosh Bagchi

\_\_\_\_\_ BCEE Examiner

Dr. Chunjiang An

\_\_\_\_\_ BCEE Examiner

Dr. Zhi Chen

\_\_\_\_\_ Supervisor

Dr. Catherine N. Mulligan

Approved by

\_\_\_\_\_ Graduate Program Director

Dr. Mazdak Nik-Bakht

\_\_\_\_\_ Dean of Faculty

Dr. Mourad Debbabi

Date: August 17<sup>th</sup>, 2022

## Abstract

### Removal of Nutrients from Water Using Micellar Enhanced Ultrafiltration Using biosurfactant

Sarjana Binte Rafiq Era

Removing nutrients, e.g., ammonia, nitrate, and phosphate ( $\text{NH}_4^+$ ,  $\text{NO}_3^-$ ,  $\text{PO}_4^{3-}$ ) from wastewater, has been a great challenge. Various studies have been undertaken for metal and nutrient removal from wastewater using physical and chemical treatment techniques and synthetic surfactants. However, there have been very few studies on treatment incorporating biodegradable biosurfactants, which are the candidates to enhance nutrient removal from wastewater. Either a microbial-derived biosurfactant (rhamnolipid) or a yeast-derived biosurfactant (sophorolipid) or both can be used for this removal process based on their efficiency with Micellar Enhanced Ultrafiltration (MEUF). In the MEUF process, surfactant micelles, aggregates of surfactant monomers, can bind cations and anions when oppositely charged. The MEUF system works by rejecting micelles containing cations and anions with larger diameters than the pore size of the ultrafiltration membrane. The MEUF process can be incorporated in this proposed study to increase the efficiency of metal removal and lower costs by reducing pore pressure compared to reverse osmosis (RO) and nanofiltration (NF). The micelle-containing metal cations will be removed, and it is possible to recover the biosurfactant from the filtration system. Different parameters, e.g., surface tension, critical micelle concentration (CMC), pH, and temperature, were examined during the experimentation. The overall efficiency of the process was estimated based on the ion concentration of the final filtrate. The experimental results demonstrate that the elimination rate for  $\text{NH}_4^+$ ,  $\text{PO}_4^{3-}$ , and  $\text{NO}_3^-$  is around 80-90% at higher temperatures and biosurfactant concentrations. Removal rates varied from 60 to 70% at lower pH and initial ionic concentrations. However, one of the system's significant disadvantages is the reduction in membrane permeate flux produced by various experiment conditions, one being membrane fouling. The optimum conditions that deliver the most excellent nutrient removal were determined. The generated results can further be used for metal and nutrient removal from eutrophic lakes, wastewater treatment plants (WWTP), and industrial effluents in future work.

## **Acknowledgments**

First and foremost, I want to convey my heartfelt gratitude to Prof. Catherine N. Mulligan, my supervisor and mentor, for her constant support of my studies and research, as well as her patience, inspiration, passion, and vast knowledge. Her advice was invaluable throughout my thesis research and writing.

I want to express my gratitude to Hong Guan and Luc Demers, the lab technician, for helping me with my experimental setup and characterization. Kaiser Mahmood, Dr. Dileep Palakkeel Veetil, and my lab companions for assisting me with the characterization analysis of my experiments and assisting with thesis writing and motivation. Finally, I would like to express my gratitude to my family for inspiring and supporting me throughout the entire journey.

## Table of Contents

List of Figures .....	viii
List of Tables .....	x
List of abbreviations .....	xi
Chapter 1: Introduction .....	1
1.1 Nutrient Pollution and Potential Solutions.....	1
1.2 Objectives .....	3
1.3 Organization of the Research Study.....	3
Chapter 2: Background and Literature Review .....	5
2.1 Nutrients.....	5
2.1.1 Causes and effects of nutrient pollution.....	5
2.1.2 Nitrates.....	6
2.1.3 Phosphates.....	6
2.1.4 Ammonia.....	7
2.2 Definition of Membrane .....	7
2.3 Membrane Separation Processes.....	11
2.3.1 Description of membrane separation .....	11
2.3.2 Membrane materials.....	13
2.3.3 Inorganic membrane materials.....	14
2.3.4 Membrane operation .....	15
2.4 General Types of Membranes Separation Processes .....	16
2.4.1 Reverse Osmosis (RO).....	16
2.4.2 Nanofiltration (NF) .....	18
2.4.3 Microfiltration.....	20
2.5 Conventional Ultrafiltration Modules .....	21
2.5.1 Tubular membrane module .....	21
2.5.2 Hollow fiber membrane module .....	21
2.5.3 Spiral wound membrane module .....	22
2.6 Membrane Flux.....	25
2.7 Factors controlling permeate flux .....	26
2.7.1 Concentration polarization.....	26
2.7.2 Membrane fouling.....	27
2.7.3 Fouling control: chemical and physical cleaning.....	28
2.8 Surfactants.....	30
2.9 Formation of Micelle .....	31
2.10 Biosurfactants .....	32

2.10.1 Sophorolipids .....	32
2.11 Enhanced Ultrafiltration.....	35
2.12 Effects of Different Factors on The Removal Process.....	36
2.12.1 Effect of applied pressure .....	36
2.12.2 Effect of surfactant concentration in the feed solution .....	37
2.12.3 Effect of feed temperature.....	37
2.12.4 Effect of metal ion concentration in the feed .....	38
Chapter 3. Materials and Methods .....	40
3.1 Materials .....	40
3.2. Instruments.....	41
3.2.1 Ultrafiltration system .....	41
3.2.2 Peristaltic pump .....	42
3.2.3 Xampler™ cartridge.....	42
3.2.4 Miscellaneous instruments.....	43
3.3 CMC of Sophorolipid .....	45
3.5 Ion Solution.....	46
3.6 Study of Transmembrane Pressure (TMP).....	47
3.7 Effect of Different pH Values.....	47
3.8 Effect of Sophorolipid Concentration .....	48
3.9 Effect of Anion and Cation Concentration.....	48
3.10 Effect of Temperature .....	49
3.11 Membrane Unit Experiments .....	49
3.12 Cleaning the Ultrafiltration Membrane.....	50
Chapter 4: Results and Discussion.....	51
4.1 CMC Determination.....	51
4.2 Significance of CMC Value.....	52
4.3 Effect of pH on Removal Rate (Ions: SL=1:1.3) .....	54
4.4 Effect of pH on Removal Rate(Ions:SL=13.5:1) .....	55
4.5 Effect of Temperature on Permeate Flux (Ions: SL=1:1.3) .....	57
4.6 Effect of temperature in Permeate Flux (Ions: SL=13.5:1).....	57
4.7 Effect of Temperature on Removal Rate (Ions: SL=1:1.3).....	58
4.8 Effect of Temperature on Removal Rate (Ions: SL=13.5:1).....	59
4.9 Effect of Initial Concentration on Removal Rate (Ions: SL=1:1.3).....	60
4.10 Effect of Initial Concentration on Removal Rate(Ions: SL=13.5:1) .....	61
4.11 Effect of Sophorolipid Concentration on Removal Rate (Ions: SL=1:1.3).....	63
4.12 Relation Between Surface Tension and Concentration of The Solution.....	64

4.13 Effect of Sophorolipid Concentration on Removal Rate (Ions: SL=13.5:1).....	65
4.14 Effect of Transmembrane Pressure in Permeate Flux(Ions: SL=1:1.3) .....	67
4.15 Effect of Transmembrane Pressure in Permeate Flux(Ions: SL=13.5:1) .....	68
4.16 Permeate flux Over Time (Ions: SL=1:1.3) .....	69
4.17 Permeate flux Over Time (Ions: SL=13.5:1) .....	69
Chapter 5: Conclusions .....	71
References.....	73

## List of Figures

Figure 2. 1 Different membrane separation processes with pore size and pressure required (Kurniawan et al., 2006). .....	12
Figure 2. 2 Schematic diagram of reverse osmosis mechanism (Ulbricht, 2006) .....	17
Figure 2. 3 Schematic diagram of the experimental setup of separation mechanism of NF membrane (Zhao et al., 2016). .....	20
Figure 2. 4 Tubular Membrane Module (Bade & Lee, 2011). .....	21
Figure 2. 5 Hollow Fiber Membrane Module (Kurniawan et al., 2006). .....	22
Figure 2. 6 Plate-and-frame modules (Bade & Lee, 2011). .....	23
Figure 2. 7 Concentration polarization model for the ultrafiltration of surfactants (Jönsson et al., 2006). .....	27
Figure 2. 8 Different types of fouling mechanisms (Ladewig & Al-Shaeli, 2017). .....	28
Figure 2. 9 Membrane Physical and chemical cleaning processes (Wang et al., 2014). .....	29
Figure 2. 10 Micelle Formation mechanism (Mungray et al., 2012). .....	32
Figure 2. 11 Molecular Structure of Sophorolipid (Zeftawy & Mulligan, 2011). .....	34
Figure 2. 12 Micellar Enhanced Ultrafiltration (Yaqub & Lee, 2019). .....	36
Figure 3. 1 Ultrafiltration system with the reservoir (G.E Healthcare, 2004) .....	41
Figure 3. 2 QuixStand Benchtop System with a peristaltic pump(G.E Healthcare, 2004).....	42
Figure 3. 3 930 Compact I.C. Flex.....	43
Figure 3. 4 Tensionmat 21 (Fisher Scientific). .....	46
Figure 4. 1 CMC Determination of Sophorolipid. ....	52
Figure 4. 2 Effect of pH on removal rate of $\text{NO}_3^-$ , $\text{PO}_4^{3-}$ and $\text{NH}_4^+$ , SL concentration= 0.3%, Temperature=22°C, $\text{NO}_3^-$ , $\text{PO}_4^{3-}$ and $\text{NH}_4^+$ concentration=100 mg/l, Molecular weight cut-off (MWCO)=10,000, TMP= 120 kPa, Flow rate =70 rpm .....	55
Figure 4. 3 Effect of pH on removal rate of $\text{NH}_4^+$ , $\text{NO}_3^-$ , $\text{PO}_4^{3-}$ , concentration of $\text{NH}_4^+$ =575 mg/L, concentration of $\text{PO}_4^{3-}$ =818.9 mg/L and concentration of $\text{NO}_3^-$ is 2042 mg/L SL concentration=0.03% and the temperature=22°C. The molecular weight cut-off (MWCO)=10,000. ....	56
Figure 4. 4 Effect of temperature on permeate flux at pH 6, $\text{NH}_4^+$ , $\text{NO}_3^-$ , $\text{PO}_4^{3-}$ = 100 mg/L SL concentration= 0.3%, temperature=22°C, molecular weight cut-off (MWCO)=10,000, TMP= 120 kPa, flow rate =70 rpm .....	57

Figure 4. 5 Effect of Temperature Pressure on Permeate Flux at pH 6, concentration of $\text{NH}_4^+$ =575 mg/L, concentration of $\text{PO}_4^{3-}$ =818.9 mg/L and concentration of $\text{NO}_3^-$ is 2042 mg/L SL concentration=0.03% and the temperature=22°C. The molecular weight cut-off (MWCO)=10,000.....	58
Figure 4. 6 Effect of temperature on removal rate of $\text{NO}_3^-$ , $\text{PO}_4^{3-}$ and $\text{NH}_4^+$ , concentration of $\text{NH}_4^+$ , $\text{NO}_3^-$ , $\text{PO}_4^{3-}$ = 100 mg/L SL concentration= 0.3%, temperature=22°C, molecular weight cut-off (MWCO)=10,000, TMP= 120 kPa, flow rate =70 rpm .....	59
Figure 4. 7 Effect of temperature on removal rate of $\text{NO}_3^-$ , $\text{PO}_4^{3-}$ and $\text{NH}_4^+$ . The initial concentration of $\text{NH}_4^+$ =575 mg/L, $\text{PO}_4^{3-}$ =818.96 mg/L and $\text{NO}_3^-$ =2042 mg/L, SL concentration=0.03%. Temperature=22°C, pH=6, membrane's molecular weight cut-off (MWCO)=10,000, TMP=120kPa .....	60
Figure 4. 8 Effect of initial concentration on removal rate of $\text{NO}_3^-$ , $\text{PO}_4^{3-}$ and $\text{NH}_4^+$ , TMP=120kPa, Temperature=22°C and the sophorolipid concentration= 0.3%. The pH was 6, molecular weight cut-off (MWCO)= 10,000. The flow rate = 70 rpm.....	61
Figure 4. 9 Effect of initial concentration on removal rate of $\text{NO}_3^-$ , $\text{PO}_4^{3-}$ and $\text{NH}_4^+$ at temperature= 22°C, sophorolipid concentration=0.03%, pH=6, MWCO=10,000, TMP=120kPa	62
Figure 4. 10 Effect of Sophorolipid on removal rate of $\text{NO}_3^-$ , $\text{PO}_4^{3-}$ and $\text{NH}_4^+$ , at ion concentration=100 mg/L and TMP=120kPa, temperature=22°C and the sophorolipid concentration= 0.3%. The pH was 6, Molecular weight cut-off (MWCO)=10,000, the flow rate = 70 rpm .....	63
Figure 4. 11 Change of surface tension in the feed and permeate solution, ion concentration=100 mg/L, sophorolipid concentration=0.4%, temperature=22°C, pH=6, MWCO=10000, TMP=120kPa, he flow rate=70 rpm .....	65
Figure 4. 12 Effect of sophorolipid concentration on removal rate of $\text{PO}_4^{3-}$ , $\text{NO}_3^-$ and, $\text{NH}_4^+$ , The initial concentration of $\text{NH}_4^+$ =575 mg/L, $\text{PO}_4^{3-}$ =818.96 mg/L and $\text{NO}_3^-$ =2042 mg/L. Temperature=22°C, pH=6, Molecular weight cut-off (MWCO) was 10,000. The flow rate of the recirculation pump was 70 rpm during the test.....	66
Figure 4. 13 Effect of Transmembrane Pressure on Permeate Flux at pH 6, $\text{NH}_4^+$ , $\text{NO}_3^-$ , $\text{PO}_4^{3-}$ = 100 mg/L, Sophorolipid = 0.3%, TMP=120kPa, temperature=22°C and the sophorolipid concentration= 0.3%. The pH was 6, molecular weight cut-off (MWCO)=10,000, the flow rate = 70 rpm .....	67

Figure 4. 14 Effect of Transmembrane Pressure on Permeate Flux at pH 6, $\text{NH}_4^+$ , $\text{NO}_3^-$ , $\text{PO}_4^{3-}$ = 575, 2042 and 818.96 mg/L and sophorolipid = 0.03%, the pH was 6, molecular weight cut-off (MWCO)=10,000, the flow rate = 70 rpm.....	68
Figure 4. 15 Effect permeate flux over time at pH 6, $\text{NH}_4^+$ , $\text{NO}_3^-$ , $\text{PO}_4^{3-}$ = 100 mg/L and sophorolipid concentration = 0.3%, TMP=120 kPa .....	69
Figure 4. 16 Effect of Permeate Flux over time at pH 6, $\text{NH}_4^+$ , $\text{NO}_3^-$ , $\text{PO}_4^{3-}$ = 575, 2042 and 818.96 mg/L and Sophorolipid = 0.03%.....	70

## List of Tables

Table 2. 1 Advantages and disadvantages of conventional treatment processes versus MBRs (Asano et al., 2007).....	9
Table 2. 2 Physical processes with examples (Kurniawan et al., 2006) .....	11
Table 2. 3 Different separation processes and a list of common materials used for long term separation (Schwarze, 2017).....	13
Table 2. 4 Membrane operation affecting factors (Abbasi-Garravand & Mulligan, 2014).....	15
Table 2. 5 Advantages and disadvantages of the different membrane modules (Schwinge et al., 2004) .....	24
Table 2. 6 Fouling Control: chemical and physical cleaning (Wang et al., 2019).....	30
Table 3. 1 Lactonic sophorolipids SL18 (Ecover, Belgium 2014). .....	40

## List of abbreviations

<b>BOD</b>	Biochemical Oxygen Demand
<b>CMC</b>	Critical Micelle Concentration
<b>IC</b>	Ion chromatography
<b>ICP</b>	Internal concentration polarization
<b>ICP-MS</b>	Inductively Coupled Plasma Mass Spectrometry
<b>MBR</b>	Membrane Bioreactor
<b>MEUF</b>	Micellar Enhanced Ultrafiltration
<b>MWCO</b>	Molecular Weight Cut Off
<b>NF</b>	Nanofiltration
<b>R<sup>2</sup></b>	Square Linear Regression
<b>RO</b>	Reverse Osmosis
<b>SL</b>	Sophorolipid
<b>SWM</b>	Spiral Wound Membrane Module
<b>TFC</b>	Thin Film Composite
<b>TMP</b>	Transmembrane pressure
<b>TSS</b>	Total Suspended Solids
<b>UF</b>	Ultrafiltration
<b>WWTPs</b>	Wastewater Treatment Plants

## **Chapter 1: Introduction**

### **1.1 Nutrient Pollution and Potential Solutions**

Nutrient pollution is one of the most critical problems facing aquatic systems globally. The problem involves multiple pollutants from multiple sources interacting in complex ways over space and time along multiple pathways, with uncertainty present at each process stage—from pollutant generation to the final ecological and economic impacts (Liu, & Lipták, 1999). Excessive nutrient loading is a massive threat to aquatic ecosystems globally, causing profound changes in aquatic biodiversity and biogeochemical processes (Ferraz et al., 2013). Due to nutrient enrichment from organic inputs and agricultural run-off, the world's sensitive, fresh waterways are in jeopardy. Despite the introduction of far-reaching environmental regulations to address human impacts on aquatic populations, the ramifications of nutrient loading for stream ecosystem functioning remain little known (Camargo & Alonso, 2006). This situation is concerning since critical ecosystem services (such as the provisioning of healthy fisheries and the decomposition of organic matter as a supporting service) rely on ecosystem processes such as leaf-litter breakdown and other nutrient-cycling activities (Miao et al., 2019). Removing different nutrients (e.g., phosphorus, nitrate, ammonium) from wastewater has been a great challenge in Montreal and elsewhere. There are numerous traditional methods for eliminating nutrients from water and wastewaters. The membrane separation technology is an innovative and appropriate technology for eliminating nutrients (Camargo & Alonso, 2006). This technique is commonly applied since it is reasonably simple to incorporate into the entire process. Because of the ion size in the aqueous phase, reverse osmosis (RO) or nanofiltration can be used to separate ions; however, these are not cost-effective procedures (Kurniawan et al., 2006). A high transmembrane pressure is required in RO membranes for a consistent permeate flux, making the

process very expensive (Mulligan et al., 2010). Out of various existing nutrient removal methods, biological additives such as biosurfactants are eco-friendly, recyclable, and proven to be more sustainable than other standard agents. Biosurfactants are renowned for their amphiphilic nature, biodegradability, low toxicity, and excellent surface-active properties. It can perform efficiently at extreme temperatures, which is a prerequisite for the treatment processes. So far, various studies have been undertaken for metal and nutrient removal from wastewater using a synthetic surfactant (Robert et al., 1989).

In contrast, very few studies have been conducted for the removal process using biosurfactants. Biosurfactants' level of pH and salinity make them excellent candidates for metal and nutrient removal from wastewater. Either microbial-derived biosurfactant (rhamnolipid) or yeast-derived biosurfactant (sophorolipid) or both can be used for this removal process based on their efficiency with MEUF (Micellar Enhanced Ultrafiltration). In the MEUF process, spherical aggregates comprising the surfactant micelles, ionic solute, and organic solute is formed by binding cations with the oppositely charged surfactant micelle (Mulligan et al., 2010). The surfactant-based MEUF has been tested to separate multivalent anions and cations (Baek et al., 2003).

In this procedure, a surfactant is added to the diluted aqueous solution. A surfactant's structure comprises a hydrophilic head and a hydrophobic tail. When the surfactant concentration exceeds the critical micelle concentration (CMC), a micelle is formed, a spherical or cylindrical clump of monomers. Due to electrostatic forces, heavy metal ions bond to the surface of oppositely charged micelles (Camargo & Alonso, 2006). Surfactants are divided into two categories: synthetic and biologically generated. Biosurfactants are biogenic surfactants produced by bacteria, yeast, and fungi. Synthetic surfactants are the result of chemical synthesis

and are derived from petrochemicals, while synthetic surfactants are the result of chemical synthesis and are derived from petrochemicals (Mulligan et al., 2001). Biosurfactants have several advantages over synthetic surfactants, including low toxicity, high biodegradability, low irritancy, and compatibility with human skin. The properties of biosurfactants are unaffected by changes in pH, temperature, or salinity (Abbasi-Garravand & Mulligan, 2014).

## **1.2 Objectives**

The main goal of this study is to develop a method for the removal of phosphorus, nitrate, and ammonium from contaminated water. For achieving this purpose, the use of biosurfactant in micellar enhanced ultrafiltration has been chosen in this study. Nutrients were removed using the biosurfactant enhanced ultrafiltration membrane process technology to achieve this. The biosurfactant used in this research was Sophorolipid SL18 for micellar enhanced ultrafiltration (MEUF) experiments. The objectives of this study are classified as follows:

- To determine the feasibility of using Sophorolipid SL18 to remove phosphorus, nitrate, and ammonium from contaminated water
- To determine the parameters that impact the system efficiency
- To evaluate the factors that influence the permeate flux and removal efficiency
- To investigate the influence of Sophorolipid SL18 on the rejection of nitrate, phosphorus, and ammonia.

## **1.3 Organization of the Research Study**

This thesis is divided into five chapters. The introduction and goals of the study are described in the first chapter. The second chapter covers nutrient properties (e.g., ammonia,

sulphate, and phosphate), membrane technology, surfactants, biosurfactants, and enhanced micellar ultrafiltration as a literature review. Chapter Three discusses the materials, apparatus, and methods utilized in the experiments. The results of the experiments are displayed and explained in Chapter Four. The fifth chapter summarizes the study's findings and introduces the recommendations for future research.

## **Chapter 2: Background and Literature Review**

Nitrogen and phosphorus are the primary nutrients to be concerned about when treated wastewater discharges. They persist in the stream that is treated biologically, requiring additional advanced treatment. Nitrogen and phosphorus discharges have been shown to accelerate lake eutrophication and increase algal growth and rooted aquatic plants in shallow streams. Besides an aesthetic issue (Kurniawan et al., 2006), it creates several problems, including depletion of dissolved oxygen in receiving waters, toxicity toward aquatic life, and increased chlorine disinfection efficiency. Additionally, nitrate, the form of nitrogen converted through nitrification, is well known for its fatal effects on infants. It is necessary to remove nitrogen and phosphorus from wastewater (Liu & Lipták, 1999) (Metcalf, 2003). Reverse osmosis (RO) or nanofiltration (NF) could be used to separate mineral nutrients ions from wastewater. However, the operating costs of RO or NF are high due to their limited permeate fluxes and requirement for high transmembrane pressure (TMP)(Kim et al., 2004). Micellar-enhanced ultrafiltration (MEUF) has been proposed as a cost-effective method for removing a variety of micropollutants at lower pressures.

### **2.1 Nutrients**

#### **2.1.1 Causes and effects of nutrient pollution**

Watershed geology and land use impact the number of nutrients entering a lake via surface water runoff. A lake, estuary, or bay slowly deteriorating during eutrophication can become a bog or marsh and eventually disappear. Some nutrients are obtained through natural processes such as the breakdown of plants and animals (Mulligan & Sharifi-Nistanak, 2016). Due to the increased amounts of nutrients such as nitrogen and phosphorus, the water body can be saturated

by excessive vegetation in the subsequent stages of eutrophication. The urbanization process, waste discharges, agricultural and residential development can accelerate the process.

Algal blooms provide a disagreeable odour and appearance, detracting from a lake's visual appeal. Fishing and swimming may deteriorate significantly, and tourism may decline as a result. Lakes with water contamination can have several adverse outcomes.

The process of plankton death and degradation requires oxygen. As a result of the lack of light, submerged plants die, decompose, and consume more oxygen. Fish and other species suffer badly and die because they cannot "breathe" because there is not enough dissolved oxygen in the water. This incident can happen close to the area of the depleted oxygen or far downstream, resulting in deteriorated estuaries, lakes, and reservoirs (Camargo & Alonso, 2006).

### **2.1.2 Nitrates**

The principal nutrients in our lakes, streams, and wetlands are phosphorus (P) and nitrogen (N). Nitrogen is required for the development of plant and animal tissue. It is mainly used to produce protein by plants and animals. Nitrogen enters the environment in a wide range of chemical forms as dissolved or particulate forms found in living and dead species' tissues. Nitrate, a dissolved ion in water, can be toxic to humans and animals in high amounts. Nitrates in water can make newborns and domestic animals sick (Camargo & Alonso, 2006).

### **2.1.3 Phosphates**

Septic systems, animal feedlots, agricultural fertilizers, manure, industrial wastewater, sanitary landfills, and rubbish dumps are all common causes of excess nitrate reaching lakes and streams. For converting sunlight into valuable energy, phosphorus is a critical nutrient. It is also essential for cell growth and reproduction (Mulligan & Sharifi-Nistanak, 2016). It is one of the twenty most abundant elements in the solar system and the eleventh most prevalent in the earth's

crust. In water, phosphorus is usually sparse in natural conditions. Researchers recognized in the 1960s that anthropogenic sources of phosphorus are a pivotal contributor to excessive algal growth and impaired lake water quality. Organic and inorganic phosphorus can be dissolved in water and sediment particles. Plants prefer inorganic phosphates, although alternative forms can be employed if phosphates are not accessible (Chen et al., 2020). Phosphorus accumulates in lake sediments (Kim et al., 2004). Although it is often inaccessible to algae when it remains in the sediments, specific biochemical and physiological processes can allow sediment phosphorus to be released into the water. For instance, bottom-feeding fish such as carp can churn up sediments which release phosphorus into the water (Camargo & Alonso, 2006).

#### **2.1.4 Ammonia**

Ammonia produces nitrogenous oxygen demand, eutrophication, and alterations in fish health in aquatic environments. Nitrogenous biological oxygen demand (NBOD) is caused by nitrification (see terrestrial effects). In nitrification, dissolved oxygen ( $O_2$ ) is utilized to react with  $NH_3$ . As a result, less  $O_2$  is accessible to species that rely on it. As in terrestrial contexts, nitrification produces nitrate, which can lead to eutrophication (Camargo & Alonso, 2006). In standing water, nitrophilous algae and macrophytes produce massive blooms (C. Wang et al., 2019). This places a strain on resources and can also damage species indirectly through the production of algae. Ammonia, on the other hand, may directly injure creatures with porous skin if they absorb it. Ammonia exposure has been associated with fish death, as well as changes in fish development, gill condition, organ weights, and red blood cell levels (Chen et al., 2020).

## **2.2 Definition of Membrane**

A membrane is a thin sheet, film, or layer that acts as a physical barrier between two liquid, gas, or vapor phases. Another way to put it is that a membrane is a transitional phase

between two adjacent phases that acts as an effective selective barrier, regulating species transport between (Kurniawan et al., 2006) the two compartments (Ulbricht, 2006). While the membrane itself can be a solid, a liquid, or a gel, it is made up of multiple layers. The membrane is thought of as a molecular sieve that is constructed in the form of a film from multiple layers of material with a fine mesh or tiny pores to allow for the separation of microscopic particles and molecules. It functions as a selective barrier, allowing specific substances to pass through while preventing others. Selectivity is the ability of membranes to distinguish species. Membranes are used to separate solutes from solvents, solutes, particles, and particles from solvents. A membrane is an intervening phase that separates two phases and acts as an active or passive barrier to constituents' transit between adjoining phases. Membranes may be porous or impermeable. The separation of a mixture of components using a porous membrane is accomplished by passing one or more components through the membrane (permeate fractions) and rejecting the remaining components (retentate fractions) "membrane" refers to an interface or discontinuity between two phases. The membrane regulates the zone through which compounds pass. Moreover, the membrane can also be defined as a barrier whose function is to prevent permeation of all compounds. The membrane can regulate the pace at which substances infiltrate (Mulder & Mulder, 1996).

Because water quality in wastewater treatment and reuse applications is crucial, advanced treatment technologies are used to achieve the desired level of effluent quality. As suggested by Asano et al. (2007), an almost endless number of treatment processes can be applied in water reuse applications to improve the quality of treated effluent for various purposes, such as different water reuse scenarios. Table 2.1 shows different processes and their capability of removing various contaminant classes. Most established wastewater treatment

processes employ biological treatment to remove BOD, total suspended solids (TSS), and even total nitrogen and phosphorus. In membrane-assisted processes, membranes have an essential role in removing residual suspended solids and improving the effectiveness of disinfection (Sadr & Saroj, 2015).

In recent years, membrane bioreactor (MBR) technology, which combines biological-activated sludge and membrane filtration, has grown in popularity, availability, and acceptance for the treatment of a wide range of wastewaters the traditional treatment processes cannot cope with either wastewater composition or flow rate fluctuations. MBR technology is also employed when the demand for effluent quality surpasses the capacity of the conventional treatment method. MBR may become an essential upgrade of existing technology to meet the legal requirements in wastewater treatment plants as we gain a better understanding of emerging pollutants in wastewater, their biodegradability, and their inclusion in new laws (WWTPs) (Sadr & Saroj, 2015).

**Table 2. 1 Advantages and disadvantages of conventional treatment processes versus MBRs (Asano et al., 2007).**

<b>Advantages of conventional treatment</b>	<b>Disadvantages of conventional treatment</b>
<ul style="list-style-type: none"> <li>Technologies are well understood</li> </ul>	<ul style="list-style-type: none"> <li>Greater sludge production</li> </ul>
<ul style="list-style-type: none"> <li>Process potentials are universally accepted</li> </ul>	<ul style="list-style-type: none"> <li>More bio-solids handling and costs required</li> </ul>
<ul style="list-style-type: none"> <li>Different configurations allow the process to be designed to maximize contact time between macromolecules and microorganisms</li> </ul>	<ul style="list-style-type: none"> <li>Clarifier performance is reduced owing to the development of filamentous organisms or poor settling sludge in the aeration process</li> </ul>

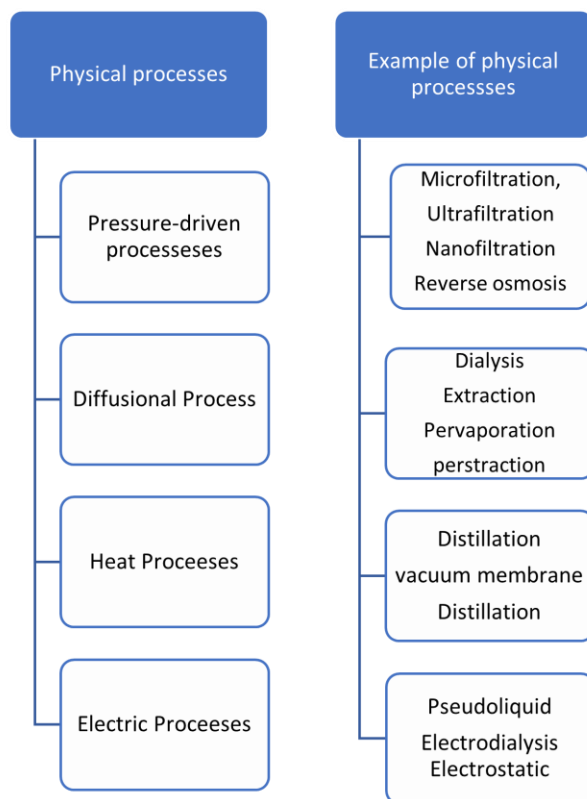
<ul style="list-style-type: none"> <li>• Skilled operation and maintenance personnel are available</li> </ul>	<ul style="list-style-type: none"> <li>• Subsequent filtration is needed for effective disinfection</li> </ul>
<b>Advantages of MBRs</b>	<b>Disadvantages of MBRs</b>
<ul style="list-style-type: none"> <li>• Nutrient removal is possible.</li> </ul>	<ul style="list-style-type: none"> <li>• Inevitable membrane fouling formation</li> </ul>
<ul style="list-style-type: none"> <li>• Low suspended solid concentration and removal of large particles leads to more effective disinfection</li> </ul>	<ul style="list-style-type: none"> <li>• Possibility of growth of specific microorganisms</li> </ul>
<ul style="list-style-type: none"> <li>• Fouling mechanism and control still under investigation</li> </ul>	<ul style="list-style-type: none"> <li>• More chemical cleaning</li> </ul>
<ul style="list-style-type: none"> <li>• Low sludge production</li> </ul>	<ul style="list-style-type: none"> <li>• More extensive pre-treatment required</li> </ul>
<ul style="list-style-type: none"> <li>• Smaller footprint and compact design</li> </ul>	<ul style="list-style-type: none"> <li>• More energy consumption</li> </ul>
<ul style="list-style-type: none"> <li>• Very high and stable effluent quality</li> </ul>	<ul style="list-style-type: none"> <li>• High capital and operation costs</li> </ul>
<ul style="list-style-type: none"> <li>• High rate of nitrification owing to longer retention of nitrifying bacteria</li> </ul>	<ul style="list-style-type: none"> <li>• No standard configuration is available</li> </ul>
<ul style="list-style-type: none"> <li>• Adaptable to decentralized and satellite Technologies</li> </ul>	<ul style="list-style-type: none"> <li>• Low oxygen transfer efficiency</li> </ul>
<ul style="list-style-type: none"> <li>• Automation is fairly achievable</li> </ul>	<ul style="list-style-type: none"> <li>• Membrane replacement is relatively expensive</li> </ul>
<ul style="list-style-type: none"> <li>• Effluent quality independence from influent quality based on buffering effect of high MLSS values</li> </ul>	<ul style="list-style-type: none"> <li>• Pilot-scale often needed for full-scale design</li> </ul>

## 2.3 Membrane Separation Processes

### 2.3.1 Description of membrane separation

Membrane separation is a process where the components of a solution are separated by a membrane that rejects undesirable substances and enables the others to pass through the membrane. In addition, the membrane's function is to alter the composition of a solution based on the relative permeation rates of the constituents (Kang & Cao, 2012). The ability of a membrane to prevent, regulate, or promote permeability can be used to assess its performance. Several elements influence the rate of penetration and the transport mechanism. There are several physical processes driven by pressure, heat, electricity, and diffusional process. Table 2.2 elaborates on different types with examples (Kurniawan et al., 2006).

**Table 2. 2 Physical processes with examples (Kurniawan et al., 2006)**



The driving force and the size of the penetrating molecule compared to the size of the accessible permeant are two factors (Robert et al., 1989). The chemical composition of the permeant and the material employed to construct the membrane (dispersive, polar, ionic) may impact the separation.

Membrane separation techniques are employed in a variety of industrial and environmental settings. Membrane separation processes can be divided into two categories: physical processes and chemical processes (Samal et al., 2017). As illustrated in Fig. 2.1, the physical processes can be categorized based on exerting a driving force (pressure, temperature, concentration, or electrical potential) across the membrane, and therefore, the chosen compounds can be transported across the membrane (Uysal & Celik, 2019) (Saleh & Gupta, 2016).

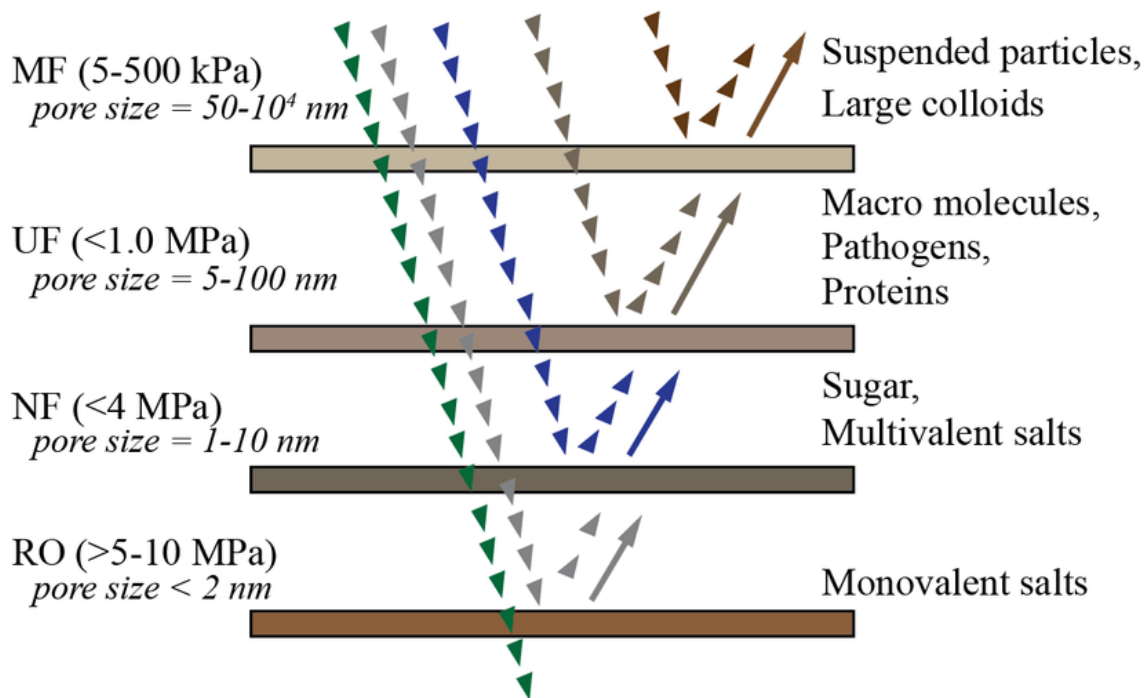


**Figure 2. 1 Different membrane separation processes with pore size and pressure required (Kurniawan et al., 2006).**

### 2.3.2 Membrane materials

The choice of materials suitable for use in the fabrication of a membrane for a specific application is a critical area that requires further investigation. The chosen membrane material enables precise control over the nature and magnitude of interactions between permeants and membranes. It determines the packing density and segment mobility of the polymer chains that make up the solid regions of the membrane, as well as the overall flexibility of the membrane. Material selection influences transport mechanism, membrane stability, and membrane performance; however, membrane preparation determines morphology, which influences permeation rate via physical properties like a steric hindrance. Membranes can be made of a variety of organic and inorganic materials. Nevertheless, most commercial membranes are made of polymers and liquids (Saleh & Gupta, 2016). Different separation procedures and a list of common materials used for long-term separation are shown in Table 2.3.

**Table 2.3 Different separation processes and a list of common materials used for long term separation (Schwarze, 2017)**

Separation process	Examples of used materials
Microfiltration	Cellulose nitrate, cellulose acetate, polyamide, polysulfone, poly (ether sulfone), polycarbonate, poly (ether imide), poly (vinylidene fluoride), polytetrafluoroethylene, polypropylene, polyacrylonitrile, regenerated cellulose
Ultrafiltration	Cellulose acetate, polyamide, polysulfone, poly (ether sulfone), polycarbonate, poly (ether imide), poly (vinylidene fluoride), polyacrylonitrile, poly (methyl

	methacrylate), regenerated cellulose
Nanofiltration	Polyamide  Dialysis  Cellulose acetate, polyamide, polycarbonate, polyacrylonitrile, poly (methyl methacrylate), regenerated cellulose
Reverse Osmosis	Cellulose acetate

Organic materials include polymer chains that make up the solid regions of the membrane. While material selection and membrane preparation procedures affect the transport mechanism, membrane stability, and performance, the latter determines the membrane morphology, influenced by physical properties such as steric hindrance (Mulligan et al., 2001). Membranes can be made of organic or inorganic materials. An example of an inorganic material is carbon. Nevertheless, most commercial membranes are made of polymers and liquids (Rahmati et al., 2017).

### **2.3.3 Inorganic membrane materials**

For gas separation, microfiltration, and nanofiltration, inorganic membranes are utilized. These membranes exhibit considerable variation in pore size, support material, and configuration (De Vos & Verweij 1998). Glass, metal, alumina, zirconia, zeolite, and carbon membranes are all similar examples. Other inorganic materials, such as silica, silicon carbide, silicon nitride, titania, cordierite, tin oxide, and mica, on the other hand, can be used to fabricate porous membranes. In general, inorganic membranes can be classified as dense (nonporous) or porous (symmetric and

asymmetric). Each of these inorganic materials has specific advantages for membrane technology applications.

Palladium and its alloys, silver, nickel, and stabilized zirconia can all be used to create dense membranes. They are used to separate gases. For instance, dense ceramic membranes separate oxygen from air or hydrogen from a mixture. Low permeability limits their industrial applications (Liu et al., 2018) (El Zeftawy & Mulligan, 2011).

Porous membranes, on the other hand, are widely used in industrial applications due to their molecular sieving properties, which include high permeability and selectivity. They exhibit high chemical stability, making them suitable for separations involving aggressive media such as acids and strong solvents (Samper et al., 2009). Additionally, they have a high thermal tolerance, making them suitable for high-temperature membrane operations. They exhibit exceptional resistance to corrosive chemicals. Emphasis is placed on porous membranes such as silica, zeolites, and carbons, which appear promising for gas separation in real-world applications (Chen & Yang 1994; Fuertes & Centeno 1995).

#### **2.3.4 Membrane operation**

Membrane operations play an essential role in performance. Table 2.4 summarizes the different types of membrane filtration and the associated operations, including concentration-driven operations, electric potential gradient operations, and temperature gradient operations (Mungray et al., 2012).

**Table 2. 4 Membrane operation affecting factors (Abbasi-Garravand & Mulligan, 2014)**

<b>Types of filtration</b>	<b>Concentration driven operation</b>	<b>Operation in an electric potential</b>	<b>Operation in a temperature gradient</b>

		<b>gradient</b>	
microfiltration	dialysis	electrodialysis fuel cell	membrane distillation
ultrafiltration	pervaporation	membrane electrolysis	
nanofiltration	forward osmosis	Electrode-ionization	
reverse osmosis	gas separation	Electro-filtration	

## 2.4 General Types of Membranes Separation Processes

### 2.4.1 Reverse Osmosis (RO)

Reverse Osmosis (RO) is a pressure-driven process in which a semi-permeable membrane (i.e., the RO membrane) rejects dissolved substances in the feeding water while permitting water to pass through (Malaeb and Ayoub, 2011). Even though reverse osmosis has been around for a long time, the application of RO as a practical separation process is a relatively new technology (Williams, 2006). The advancement of RO technology is highly dependent on the development of RO membranes, as the membrane is critical to the process's technological and economic effectiveness. Indeed, it was not until Loeb and Sourirajan invented a method for fabricating asymmetric cellulose acetate membranes with a relatively high water flux and separation factor in the early 1960s (Loeb and Sourirajan, 1962) (Kang & Cao, 2012), and particularly the subsequent invention of thin-film composite (TFC) aromatic polyamide

membranes prepared via interfacial polymerization (Cadotte et al., 1980), that RO became both feasible and economical. Recent advances in the research and use of energy recovery systems, such as the Pelton wheel, turbocharger, pressure exchanger, and Grundfos Pelton wheel (Avlonitis et al., 2003), have resulted in significant reductions in energy consumption and operation costs, thereby increasing the competitiveness of RO technology. Currently, the majority of commercially available RO membranes are asymmetric cellulose (cellulose acetate, triacetate, cellulose diacetate, or a combination thereof) or TFC. Figure 2.2 shows a schematic diagram of the reverse osmosis system.

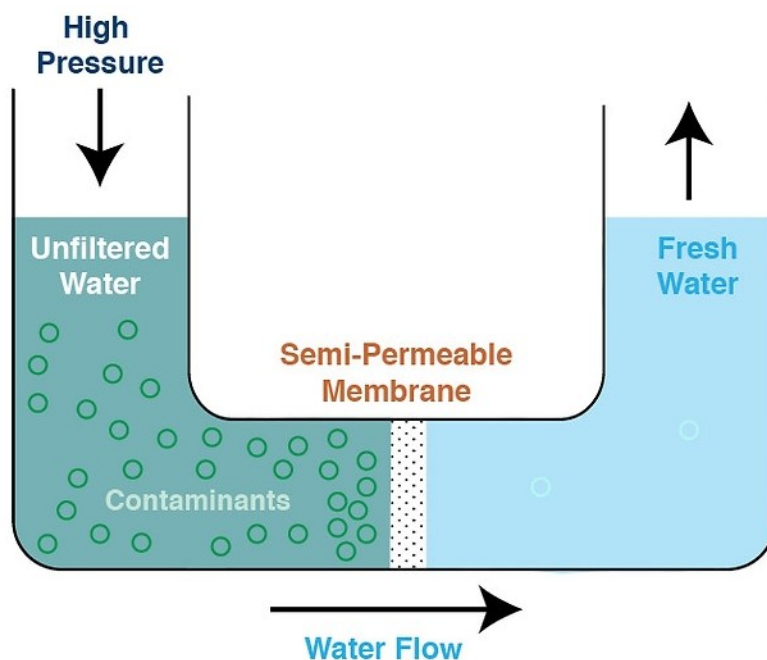


**Figure 2. 2 Schematic diagram of reverse osmosis mechanism (Ulbricht, 2006)**

The asymmetric RO membrane is made by reverse phase technology, whereas the RO TFC membrane is manufactured using an interface polymerizing approach to generate a dense, aromatic polyamide barrier layer on a microporous base such as polysulfone (Petersen, 1993). Compared to cellulose membranes, the TFC aromatic polyamide membrane has a higher water

flux. Salt rejection is more resistant to pressure compaction, has a wider operating temperature and pH range, and is more resistant to biological attack (Li and Wang, 2010). As a result, it currently dominates the RO membrane field. TFC polyamide RO membrane is prone to fouling, which is one of the factors that has prevented it from being widely used despite its numerous advantages (Subramani and Hoek, 2010). Fouling is a process that causes flux decline or impairs the quality of water produced by solute or particulate matter in feeding water to the RO-surface membrane (Wang et al., 2019). While it is possible to partially restore the performance of fouled RO membranes using the right cleaning approach (Ang et al., 2006; Creber et al., 2010), this would undoubtedly increase operation difficulty and shorten the membrane's life, resulting in increased expenses (Kang & Cao, 2012).

#### **2.4.2 Nanofiltration (NF)**

In water treatment, the nanofiltration (NF) membrane is a kind of pressure-driven membrane having characteristics that fall between those of reverse osmosis (RO) and ultrafiltration (UF) (Zhao et al., 2016). Inexpensive operation pressure, high flux, high retention of multivalent anion salts, an organic molecular over 300, comparatively low investment, and low operation and maintenance expenses are only a few of the benefits of NF. Because of all these benefits, the usage of NF has grown across the world (Lu et al., 2002). As a result, the high pressures employed in RO in the past led to a significant energy expense. The development of membranes with reduced rejections of dissolved components while maintaining improved water permeability would be a significant step forward in separation technology (Fu et al., 2012). Low-pressure RO membranes like this are referred to as NF membranes (Van der Bruggen & Vandecasteele, 2003). NF had established itself by the second part of the 1980s, and the first applications were recorded (Conlon & McClellan, 1989) (Schaep et al., 1998). The uses of NF

membranes in-ground, surface, and wastewater treatment, as a pretreatment or desalination, fouling, and the separation process, and modeling of NF membranes were reviewed in this article. Furthermore, the use of atomic force microscopy (AFM) to examine the morphology of NF membrane surfaces will be discussed (Hilal et al., 2004).

### Separation mechanism with NF membranes

NF includes removing unloaded nanoscale components with load effects from solution to the membrane surface. Uncharged components are removed due to size exclusion or variations in diffusion rates in a nonporous structure (El Zeftawy & Mulligan, 2011), which are influenced by molecule size (Brugg et al., 2003). On the other hand, the charge effect removes (mostly multivalent) ions, whereas the former removes uncharged organic species. Therefore, the performance of NF memorandum separation may be recognized in the sieving effect (steric hindrance) and the Donnan effect (electrostatic) (Wang et al. 2002). (Hilal, 2004). The nanofiltration system is schematically depicted in Figure 2.3.

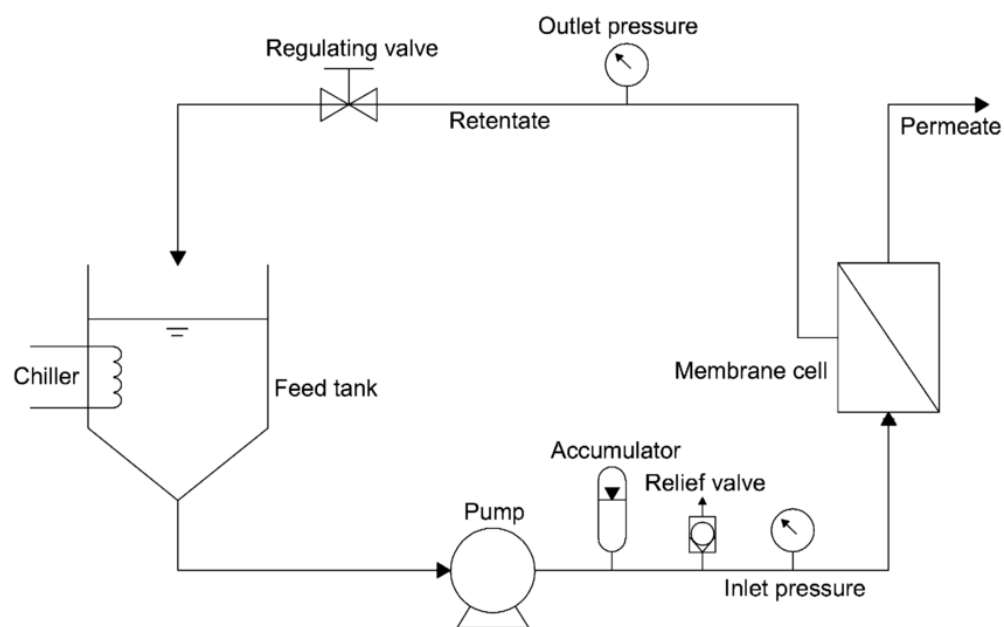


**Figure 2. 3 Schematic diagram of the experimental setup of separation mechanism of NF membrane (Zhao et al., 2016).**

### **2.4.3 Microfiltration**

Microfiltration (MF) is a pressure-driven separation technique that is frequently used to concentrate, purify, or separate macromolecules, colloids, and suspended particles from solution. The nominal pore diameters of MF membranes are generally in the range of 0.1–1.0  $\mu\text{m}$ . In the food sector, MF processing is frequently utilized for applications such as wine, juice (Wang et al., 2014), and beer clarity, wastewater treatment, and plasma separation for medicinal and commercial purposes. MF is used in biotechnology companies for applications such as cell recycling and harvesting, protein extraction from cell debris, and process stream purification (Yaqub & Lee, 2019).

MF is often operated in a cross-flow mode at relatively low TMPs (4 bar or 0.4 MPa). The feed stream is tangential to the membrane surface to avoid cake development and, therefore, membrane fouling. Cross-flow MF operation is frequently constrained by membrane fouling produced by suspended particles in the input stream. As trapped particles collect on and within the membrane, permeate flow diminishes with time. External fouling or cake formation of cells, cell debris, or other rejected particles on the surface of the membrane is often reversible. In contrast, deposition and adsorption of tiny particles or macromolecules within the membrane's internal pore structure (internal fouling) are frequently irreversible (El Zeftawy & Mulligan, 2011) (Yaqub & Lee, 2019). The decrease of effective pore area or pore counts in heavily fouled membranes might result in fluxes that are smaller than those reported in UF (Charcosset, 2012).

## 2.5 Conventional Ultrafiltration Modules

### 2.5.1 Tubular membrane module

There are a variety of methods for constructing membranes in a tubular configuration. If the membrane is located on the inside surface of a cylinder, it is referred to as a tubular module, and it is seen schematically in Fig. 2.4. Ultrafiltration is the primary use for this setup. Tubular membranes, in addition to their rigid structure (El Zeftawy, 2007), offer the benefit of being able to handle large suspended particle concentrations without clogging.

Tubular membranes are ideal for metalworking greasy waste, industrial wastewater reduction, and recovery (Wang et al., 2019).

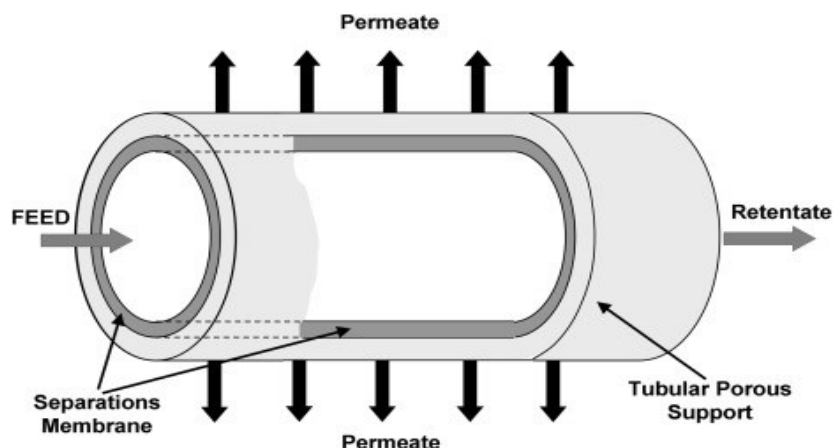


**Figure 2. 4 Tubular Membrane Module (Bade & Lee, 2011).**

### 2.5.2 Hollow fiber membrane module

Hollow fiber membranes are one of the most widely utilized membranes in the industry. Typically, a hollow fiber is coated on the exterior of porous fiber support, as seen in Fig. 2.7. Hollow fiber modules typically have a diameter of 4–8 in. (10–20 cm) and a length of 3–5 ft (1.0–1.6m). Often, the membrane is applied to the outer fiber using a dip procedure that dissolves the polymer membrane in a solvent. While Fig. 2.7 depicts the feed stream inside the

fiber, it is more frequently located on the outside of the fiber to pressurize the membrane against the porous support (Valeri et al., 1992). Bundling these fibers together is accomplished by binding the strands together at their ends, as seen in Fig. 2.5.

It has a few drawbacks, such as fouling of the hollow fiber membranes that are more prevalent than fouling other membrane designs. Contaminated input will accelerate membrane fouling, particularly in hollow fiber membranes (Uysal & Celik, 2019). Due to the manufacturing process, the hollow fiber system is more costly than other membrane systems currently on the market. High temperatures and corrosive gases may harm the hollow polymer fiber and the porous support during usage. Modules made of hollow fibers are frequently utilized in gas separation and pervaporation systems ((Uysal & Celik, 2019).

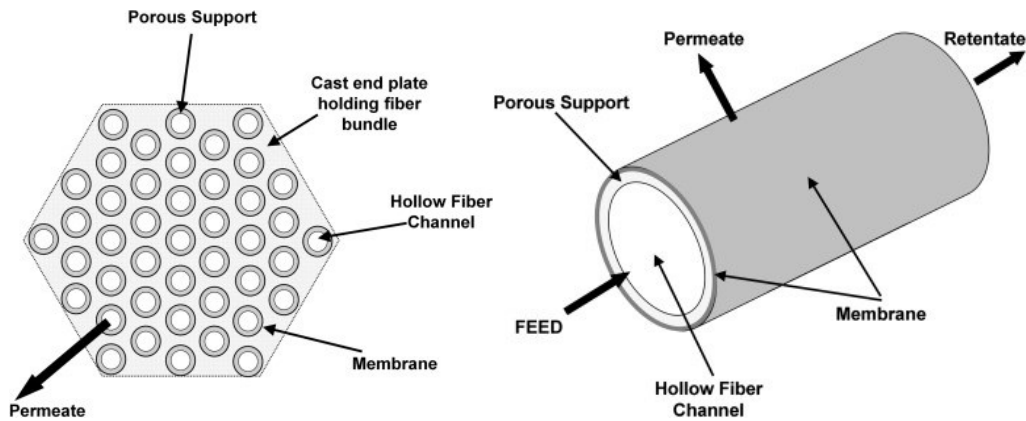


**Figure 2. 5 Hollow Fiber Membrane Module (Kurniawan et al., 2006).**

### 2.5.3 Spiral wound membrane module

As illustrated in Fig. 2.6, industrial spiral wound modules include multiple membrane envelopes, each with a surface area of 1 to 2 m<sup>2</sup>, wrapped around the central collecting pipe. The multi-envelope design reduces the pressure drop experienced by the permeate as it travels toward the center pipe. As a standard, industrial spiral wound modules are 8 inches in diameter and 40 inches in length. Within a tubular pressure vessel, the module is inserted. As illustrated in Fig.

2.6, the feed solution travels across the membrane surface (Silva et al., 2010). A part of it penetrates the membrane envelope, spiraling toward the center and exiting via the collecting tube (Baek et al., 2003).

In most cases, four to six spiral wound membrane modules are linked in series within a single pressure vessel. The membrane area of a typical 8-in.-diameter tube comprising six modules is about 100–200 m<sup>2</sup> (Figoli et al., 2009).

SWMs are used for various purposes, including desalination, water treatment, water reclamation, industrial wastewater treatment, product treatment in the dairy sector, and product recovery in the pharmaceutical industry. Concentration polarization, fouling, and significant pressure loss are the primary issues with an SWM (Schwinge et al., 2004).

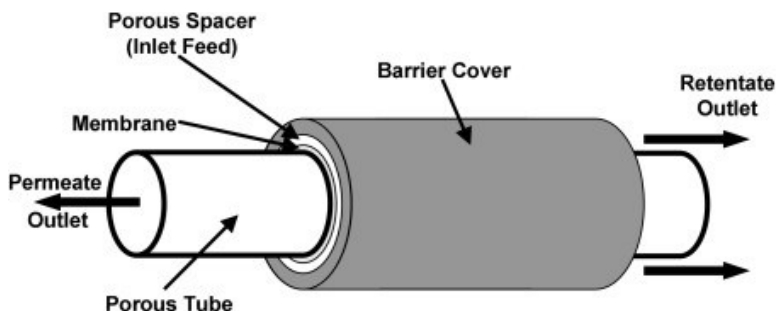


**Figure 2. 6 Plate-and-frame modules (Bade & Lee, 2011)**

Plate-and-frame modules can be built and developed in a variety of orientations, sizes, and forms, ranging from lab-scale devices that accommodate a single, small-size membrane to systems that accommodate several membranes in plate-and-frame modules (Fig. 2.8). The absence of an appropriate membrane support and poor packing density of plate-and-frame modules are two significant drawbacks. Insufficient membrane support restricts operation to low hydraulic pressures or pressures similar on both sides of the membrane (requiring relatively high process control). Low packing density results in a more extensive system footprint, more outstanding capital and operational expenses, and lower system performance (labor for

membrane replacement) (Schwarze, 2017). The other drawbacks of the plate-and-frame design are internal and exterior sealing difficulties, difficulty monitoring membrane integrity, and a limited range of working circumstances (for example, flow velocities and pressures) (Cath et al., 2006; Nayak and Rastogi, 2010b) (Shekhar et al., 2015).

The plate-and-frame arrangement involves stacking flat membranes with porous separators on top of one another. The feed's suspended solids content determines the spacing. Feed is gathered at membrane support plates which enter from one end. This module is simple to use and to detect and replace membrane flaws. Their low packing density limits their usage to small-scale applications. These flat-sheet membranes are packed together and supported by a metal structure in the feed medium. Permeate penetrates through the membrane's outer surface into the flat sheet channels and is collected at the membrane's ends. These modules can be stacked to enhance productivity (Puasa et al., 2011). The submerged module consumes less energy than the contained module due to reduced pressure-driving force needs. As they are made and sealed sheet by sheet, membranes may be readily changed. Because they can tolerate large suspended particle feeds, they are widely employed in MBRs to treat wastewater (Figoli et al. 2001). Table 2.5 summarizes the relative benefits and drawbacks of the membrane module.

**Table 2.5 Advantages and disadvantages of the different membrane modules (Schwinge et al., 2004)**

Module	Advantage	Disadvantage	Technology
Plate and frame	<ul style="list-style-type: none"> <li>• Variety of choices</li> <li>• Less energy required</li> </ul>	<ul style="list-style-type: none"> <li>• High cost</li> <li>• Time consuming process to replace</li> </ul>	MF, UF, RO

Hollow Fiber	<ul style="list-style-type: none"> <li>• Very compact system</li> <li>• The low capital cost involved</li> <li>• Back flushable</li> </ul>	<ul style="list-style-type: none"> <li>• Prone to fouling</li> <li>• Unsuitable for viscous system</li> <li>• Less availability of the product</li> </ul>	MF, NF, UF, RO
Spiral wound	<ul style="list-style-type: none"> <li>• Compact system</li> <li>• Variety of size range</li> <li>• Low capital cost</li> </ul>	<ul style="list-style-type: none"> <li>• The dead spot might be present</li> <li>• Backflushing not possible</li> </ul>	NF, UF, RO
Tubular	<ul style="list-style-type: none"> <li>• A feed with a high concentration of suspended solid can pass</li> <li>• Mechanical cleaning is easy.</li> </ul>	<ul style="list-style-type: none"> <li>• High energy required</li> <li>• High capital cost</li> <li>• Spacious arrangement required</li> <li>• High hold up</li> </ul>	MF, NF, UF, RO

## 2.6 Membrane Flux

The permeate flow rate, measured in gallons per square foot of membrane area per day, determines the rate of membrane surface fouling (GFD). Fouling occurs at a lowest rate when the flow rate decreases (Fu et al., 2017). Solutes are pulled more towards the direction of the pores with greater filtration flux, resulting in pore blockage and a cake layer on top of the membrane surface. The optimal flow is low enough to prevent deposition on the membrane's surface. Selection is based on the critical flux concept, which states that at startup, there is a flux below which no further flux decrease occurs; above it, fouling occurs (Field et al. 1995). This flow is

known as the critical flux, and its value is determined by hydrodynamics and perhaps other factors (Kim et al., 2004). The critical flux level is determined by a variety of factors, including cross-flow velocity, membrane type, solute type, and solute bulk concentration (Saleh & Gupta, 2016).

## 2.7 Factors controlling permeate flux

### 2.7.1 Concentration polarization

Concentration polarization is associated with the continual transit of contaminated influents to the membrane surface and the selective retention of specific components, resulting in the concentration of certain solutes on or near the membrane surface. Their concentration rises during the operation, resulting in forming a more concentrated boundary layer. In this layer, the fluid seems almost entirely stagnant, and the velocity at the membrane surface is zero. This indicates that diffusion is the only method of transport inside this layer (Samal et al., 2017). The concentration build-up causes a particle back-transport flow into the bulk. Cross-flow filtration can improve particle back-transport and foul by increasing the flux, which results in increased diffusion (Sadr & Saroj, 2015). Figure 2.7 shows a representation of concentration polarization.

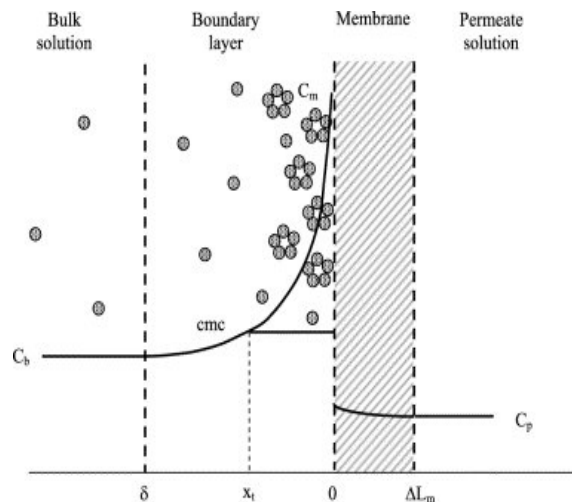


**Figure 2. 7 Concentration polarization model for the ultrafiltration of surfactants (Jönsson et al., 2006).**

### **2.7.2 Membrane fouling**

Membrane fouling is a process in which particles, colloidal particles, or solute macromolecules are deposited or adsorbed onto membrane pores or surfaces by physical and chemical interactions or mechanical action, resulting in smaller or closed membrane pores. Membrane fouling can result in significant flux decreases and a reduction in the quality of the water generated. Excessive fouling may necessitate a thorough chemical cleaning or membrane replacement. This raises a treatment plant's operational expenses. Pore blockage, pore constriction, and cake formation have all been proposed as mechanisms for membrane fouling in the past. Biological (bacteria, fungi), colloidal (clays, flocs), scaling (mineral precipitates), and organic foulants are all examples of foulants (oils, polyelectrolytes, humic acids) (Robert et al., 1989).

Membrane fouling is influenced by several parameters, including (1) particle or solute size; (2) membrane microstructure; (3) interactions between membrane, solute, and solvent; and (4) membrane surface roughness, porosity, and other physical features. As a result, membrane fouling must be prevented to maximize the life of the membrane by (1) selecting acceptable membrane materials; (2) configuring the membrane; (3) pre-treatment of raw materials; (4) optimizing operating conditions; (5) controlling inorganic salt solubility; (6) frequent rinsing of the membrane; (7) using a disinfectant; (8) raising feed water temperature; and (9) adequate maintenance (Liu et al., 2018). Figure 2.8 represents various fouling mechanisms (Sadr & Saroj, 2015).

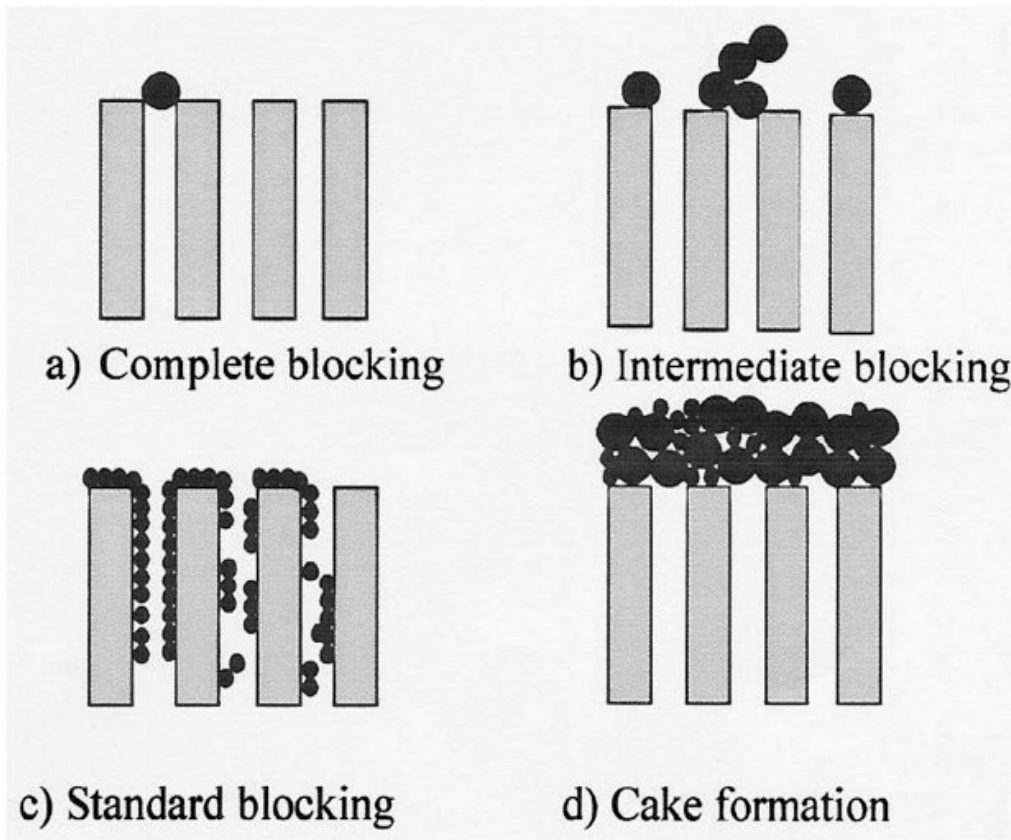


**Figure 2. 8 Different types of fouling mechanisms (Ladewig & Al-Shaeli, 2017).**

### **2.7.3 Fouling control: chemical and physical cleaning**

Physical and chemical cleaning methods are used to clean membranes. Membrane-assisted technologies, backwashing, and relaxation in wastewater treatment are commonly used for physical cleaning.

Backwashing is the process of reversing the flow toward membranes, whereas relaxation is the act of pausing permeation in order to scour the membrane with aeration (air bubbles). Chemical cleaning, on the other hand, is performed using a combination of mineral and organic acids, caustic soda, and sodium hypochlorite (Hilal et al., 2004). Occasionally, washing can be accomplished by backwashing with a reduced concentration of a chemical agent (chemically enhanced backwash) (Makkar & Cameotra, 1999). Physical cleaning is accomplished by the use

of air scouring, backwashing, and filter relaxing techniques during periods of low input when the installed capacity is decreased by 12.5%. Physical and chemical cleaning techniques of the membrane are depicted in Figure 2.9.

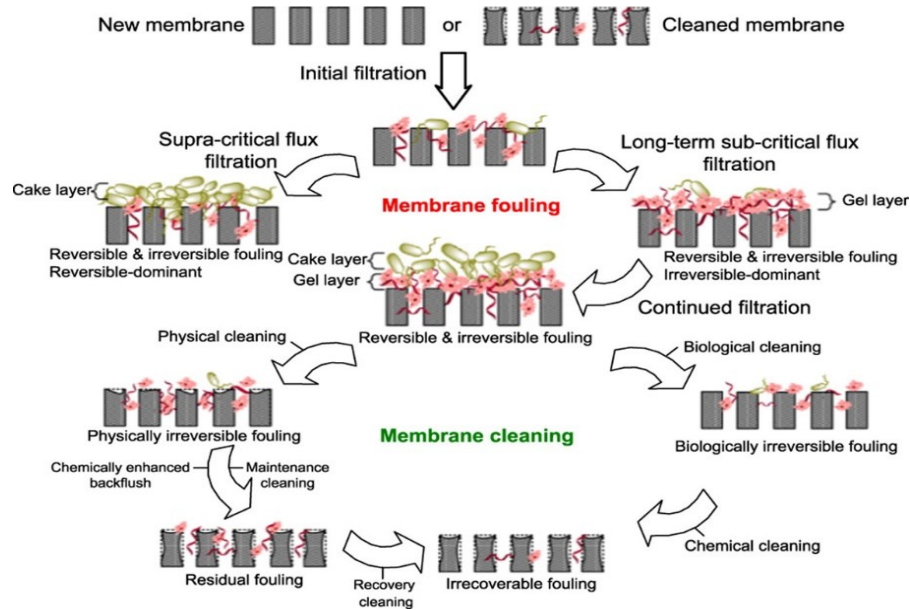


**Figure 2. 9 Membrane physical and chemical cleaning processes (Wang et al., 2014).**

Chemical cleaning is accomplished by the use of backwashing with chemical cleaning agents for routine maintenance cleaning in place in biomass and/or on-air, as well as for occasional extensive cleaning outside of the plant's operating environment (Liu et al., 2018). Table 2.5 illustrates various membrane cleaning procedures and their benefits.

Fouling control is determined in most membrane-assisted technologies by regulating flow, physical and chemical cleaning, and CP control. Controlling and minimizing CP-related fouling requires two distinct approaches (Kurniawan et al., 2006). By increasing turbulence, the boundary layer's thickness is reduced. The reduced flow results in less fouling on the membrane surface. The following summarizes a successful MBR project at the Nordkanal wastewater treatment plant in Germany (Blastakova et al., 2009).

**Table 2. 6 Fouling Control: chemical and physical cleaning (Wang et al., 2019)**

	Physical cleaning	Chemical cleaning
Methods	Backwashing without air	Base (e.g., caustic soda, citric, oxalic)
	Backwashing with air	Acid (e.g., hydrochloric/sulphuric, citric/oxalic)
	Relaxation	Oxidant (e.g., hydrogen peroxide, hypochlorite)
Advantages	Simpler and less complex	Much higher cleaning efficiencies (generally)
	No chemical is needed; consequently, no chemical waste	Capable of returning flux to original or better conditions
	No membrane degradation	Capable of removing tenacious materials from the membrane surface
	Capable of removing gross solids	

## 2.8 Surfactants

Since the concentration is higher in interfacial areas, a surfactant receives its name from a surface-active agent. Surfactants have an amphiphilic structure. A molecule with an amphiphilic structure has both hydrophilic and hydrophobic sections. In other words, their structure is divided into two parts: the head, which is polar or ionic hydrophilic, and the tail, which is nonpolar hydrophobic. An anionic, cationic, zwitterionic, or non-ionic head can be used (West and Harwell, 1992) (Ladewig & Al-Shaeli, 2017). Another categorization of surfactant is

based on the balance of the various portions of the molecule, such as hydrophilic and hydrophobic or lipophilic. A lipophilic substance is hydrophobic yet has a high affinity for fatty or organic solvents. (Abbasi-Garravand & Mulligan, 2014). Surfactants are utilized in subsurface remediation based on their environmental chemistry, hydrology, and transport processes (West and Harwell, 1992). Surfactants lower surface and interfacial tension. They can help to facilitate the transfer of organic pollutants from soils to washing solutions. Surfactants can also be utilized as flocculants, wetting agents, and foaming agents (Mulligan et al., 2001). Surfactant molecular weights range from 200 g/mole to 2000 g/mole (Li, 2009).

## **2.9 Formation of Micelle**

A single-unit surfactant molecule is known as a surfactant monomer. As the concentration of surfactant rises, the concentration of monomers rises as well until micelles form. This lowest concentration is denoted by the critical concentration of micelle, or CMC (Rosen, 1978). Every surfactant has a distinct CMC, ranging from 0.1 to 10 mM. The number of monomers remains constant at concentrations equal to or greater than CMC. As a result, the additional surfactant molecules clump together and form micelles. The hydrophobic tail of the micelles will point towards the interior in aqueous circumstances, whereas the hydrophilic head will point towards the aqueous solution (Li, 2009). When the concentrations of amphiphilic molecules exceed CMC, supramolecular structures such as micelles, bilayers, and vesicles develop (Lin, 1996). Micelle formations are spherical, elongated, cylindrical, and rodlike, depending on the system parameters (Nguyen et al., 2008). With the hydrophobic and hydrophilic ends of the surfactant, Figure 2.10 depicts the Micelle Formation process.

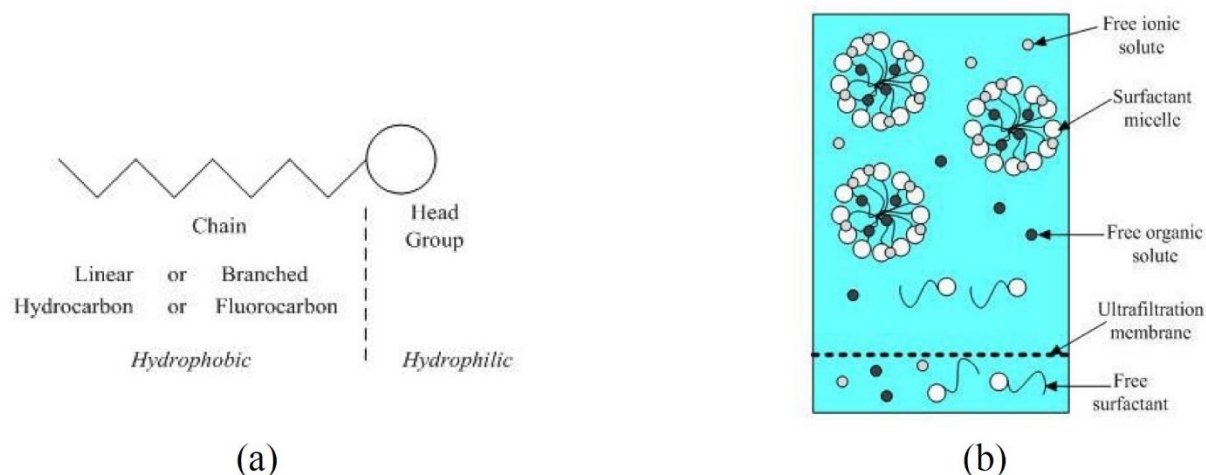


**Figure 2. 10 Micelle Formation mechanism (Mungray et al., 2012).**

## 2.10 Biosurfactants

Microbial surface-active chemicals are a category of structurally varied molecules produced by various bacteria. They are characterized primarily by their chemical structure and microbial origin. They contain a hydrophilic end made up of acid, peptide cations or anions, mono-, di-, or polysaccharides, and a hydrophobic end made up of unsaturated or saturated fatty acid hydrocarbon chains. These structures provide a variety of features, including the capacity to reduce liquids' surface and interfacial tensions and to create micelles and microemulsions between two distinct phases (Rosenberg and Ron, 1997; Smyth et al., 2010). Glycolipids are the most extensively researched microbial surfactants. Rhamnolipids, trehalolipids, sophorolipids, and mannosylerythritol lipids are the most well-known of these molecules (MELs) (Maier and Soberón-Chávez, 2000).

### 2.10.1 Sophorolipids

Sophorolipids (SL) are biosurfactants composed of both anionic and nonionic glycolipids. *Candida bombicola* has been identified as the predominant generator of SL among

these yeasts. *Candida sp.* yeasts are recognized as the principal producers of these biosurfactants (Cavalero & Cooper, 2003). These non-pathogenic yeasts can produce large quantities of SL when given vegetable oils and sugars as carbon sources (Mulligan, 2005). *Candida bombicola* can generate up to 400 g/L of sophorolipids under 33 optimal circumstances (Bogaert et al., 2011). Sophorolipids are a viable competitor with rhamnolipids for use in many applications due to their high production rate and, thus cheaper production cost (Samal et al., 2017).

According to Van Bogaert et al. (2007), the present production cost of sophorolipids varies between 2 and 5 €/kg depending on the substrates utilized and the production scale. Ashby et al. (2013) estimated that the production rate could be 90.7 million kg/year utilizing glucose and oleic sunflower oil/oleic acid at the cost of US\$2.95/kg. The structure of sophorolipids varies according to the producer strain (Van Bogaert et al., 2011) and the yeast substrate (Cavalero & Cooper, 2003). Cavalero and Cooper (2003) demonstrated that, while these yeasts require carbohydrate substrates for survival and sophorolipid formation, production rates rise when a hydrophobic substrate is added. Acidic sophorolipids (anionic surfactants) and lactonic sophorolipids make up raw sophorolipids (nonionic surfactants). The ratio of these two congeners is the substrate- and environment-dependent (Baccile et al., 2013; Weber et al., 2012; Hirata et al., 2009). The molecular structure of the sophorolipid is represented in Figure 2.11.

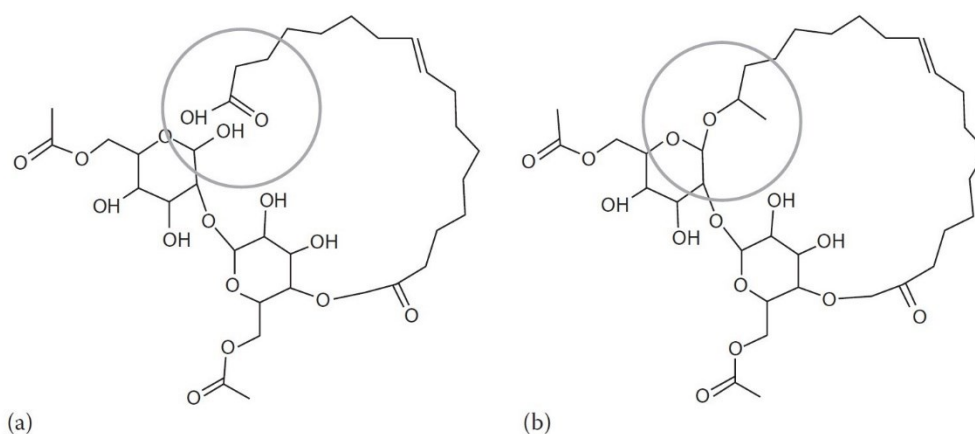


**Figure 2. 11 Molecular Structure of Sophorolipid (El Zeftawy & Mulligan, 2011).**

The varieties and ratios of the congeners determine the sophorolipid solutions' physicochemical properties. Acidic sophorolipids are made up of a glucose disaccharide head (sophorose) and a hydrophobic portion of hydroxylated fatty acids (oleic acid) linked together by an ether bond. Along with the presence of free carboxylic acid groups, this structure results in increased foam generation and solubility for acidic SL. On the other hand, Acidic sophorolipids are more sensitive to environmental changes (Baccile et al., 2013). Lactonic sophorolipids are formed when the carboxylic group in the hydrophobic tail esterifies with the hydroxyl group in the hydrophilic head (Morya and Kim, 2014). Lactonic sophorolipids have a greater capacity for reducing surface tension and exhibit increased antibacterial and antifungal activity (Van Bogaert et al., 2011; Yuan et al., 2011). Lactonic sophorolipids have been demonstrated to effectively suppress the growth of various cancer cells, including K562 cells that cause leukemia (Chen et al., 2015).

Antimicrobial activity has been observed in sophorolipids, primarily against gram-positive bacteria strains (Ashby et al., 2011). This feature enables the biosurfactant to be used in a variety of new applications. Even though sophorolipids have demonstrated success in a number of commercial applications, the higher cost of sophorolipid manufacturing, when compared to

the cost of synthetic surfactant production, is the primary barrier to their widespread adoption in the industry (Ashby et al., 2013). According to Hirata et al. (2009), sophorolipids are incredibly safe and biodegradable. According to the conventional biodegradation test, 61% of the sophorolipids decomposed after eight days of culture in their trials. These findings classified sophorolipids as quickly biodegradable compounds (Hirata et al., 2009).

At 20°C, sophorolipids reduce the surface tension of the water from 73 to 30–40 mN/m, depending on their ratio and the length of their hydrophobic tails. They are active in a wide range of temperatures, acidic to neutral conditions, and salinity levels. These properties, together with the low critical micelle concentration (CMC) of sophorolipids, their high rate of manufacturing, high biodegradability, and low toxicity, make these biosurfactants excellent candidates for application in a wide array of uses and industries (Van Bogaert et al., 2011).

## **2.11 Enhanced Ultrafiltration**

Micellar enhanced ultrafiltration is a technique for separating metal ions, organic contaminants, and inorganic compounds from aqueous streams using a membrane. Surfactants are supplied to the aqueous stream at concentrations equivalent to or higher than their critical micelle concentrations in this process (CMCs). The critical micellar concentration is the lowest micellization occurs (CMC). Surfactant monomers will assemble and form aggregates termed micelles at this surfactant concentration. Electrostatic or Van der Waals forces cause metal ions and organic molecules to dissolve in micelles. This micelle solution is subsequently filtered via an ultrafiltration membrane with an acceptable molecular weight cut-off (MWCO) size. Therefore, the ultrafiltration membrane can remove the micelles carrying the soluble

contaminants. (Misra et al. 2010). Micellar Enhanced Ultrafiltration is depicted in Figure 2.12.

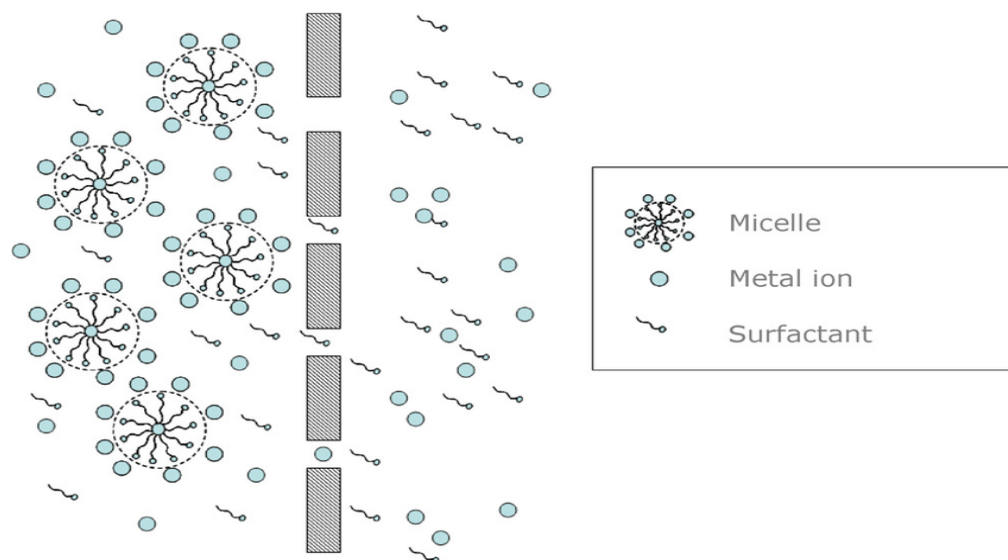


**Figure 2. 12 Micellar Enhanced Ultrafiltration (Yaqub & Lee, 2019).**

In general, the retention coefficient of the eliminating pollutant increases as the surfactant concentration increases up to CMC in MEUF (Zaghbani et al., 2009). MEUF has several advantages, including cheap operating costs, high removal efficiency, and high permeate volume flux, to name a few. In a nutshell, this system incorporates reverse osmosis' high selectivity with ultrafiltration's high flux. MEUF is utilized to remove heavy metals because of these features (Baek & Yang, 2004). Two sorts of mechanisms can be used to carry out the MEUF process.

## 2.12 Effects of Different Factors on the Removal Process

### 2.12.1 Effect of applied pressure

Cross-flow filtration is a separation technique in which the feed travels parallel to the membrane surface. Solids in the feed are caught in the membrane, and the filtrate is discharged at the bottom (Deriszadeh, 2009). The name "cross-flow filtration" comes from the fact that most of the feed flow passes across the filter surface rather than through it (Shi et al.). It has advantages over tangential flow; for example, retentate is washed away during the filtration process,

allowing a filter unit to operate for extended periods. In contrast to batch-wise dead-end filtration, it can be a continuous process (Bade & Lee, 2011).

### **2.12.2 Effect of surfactant concentration in the feed solution**

In the case of a constant surfactant concentration, the permeate flux varies by applied pressure. This could be because the operating pressure between retentate and permeate was the process's effective driving force. Increases in this parameter could overcome osmotic pressure and resistance (micelle aggregation layer (MAL)), causing more solution to filter past the membrane, increasing permeate flux (Baeurle & Kroener, 1992). Micelle concentration near the membrane surface increases at CMC (Namaghi & Mousavi, 2014). As a result, additional sites for metal ion attachment are accessible, increasing rejection. Depending on the membrane's capacity for withstanding pressure, the pressure should be changed (Schmitt, 1992, Ahmad & Puasa, 2007, Puasa et al., 2011).

### **2.12.3 Effect of feed temperature**

The permeate flux rises linearly with temperature for pure water and surfactant solution. As the temperature rises, the permeate flux increases due to the thermal expansion of the membrane material and the solution's decreased viscosity. However, larger concentration polarization was observed due to the enhanced flux (Yenphan et al., 2010). Since the surfactant CMC is a function of temperature, the temperature is the most critical parameter for MEUF (Hilal et al., 2004). Because the palisade layer of the micelle was disrupted during the demicellization process, the surfactant's CMC increased as the temperature rose (Deriszadeh, 2009). With increasing CMC values, the Kraft point likewise increases surfactant resistance. Researchers have examined how the surfactant micelle can be readily dissociated at high temperatures and reduce the number and size of a micelle. More micelle monomers travel

through the membrane (Puasa et al., 2011).

#### **2.12.4 Effect of metal ion concentration in the feed**

In the absence of a surfactant and at high ion concentrations, the permeate flux falls as the ion concentration in the feed increases. This could be because a rise in osmotic pressure opposes the permeate flux as the concentration difference across the membrane rises. Increases in cation concentration reduce repulsive interactions between head groups, making micelle formation easier. As the concentration increased, more surfactant molecules were present in micelle form, resulting in increased surfactant retention (Moreno et al., 2022).

There are various convenient ways to remove nutrients from water and wastewater. Various research has been conducted utilizing physical and chemical treatment methods to remove nutrients and non-metal ions from wastewater. Membrane separation technology is a new and efficient way to remove nutrients. This method is frequently utilized since it is simple to incorporate into the whole procedure. Because of the ion size, reverse osmosis (RO) or Nanofiltration (NF) can be used to separate ions in the aqueous phase; however, they are not cost-effective processes. RO membranes require high transmembrane pressure for a continuous permeate flux, making the process expensive (Bade & Lee, 2011).

On the other hand, surfactant incorporation in membrane technology significantly reduces system costs while increasing system efficiency. Ion removal from wastewater using a synthetic surfactant such as CTAB, CPC, and others has been studied in the past (Peng et al., 2020). However, there has been very little research on the use of biosurfactants in the elimination process. Biosurfactants' pH and salinity make them ideal for removing metals and nutrients from wastewater. For this removal process, either microbial-derived biosurfactant (rhamnolipid) or

yeast-derived biosurfactant (sophorolipid), or both can be employed, depending on their efficiency with MEUF (Micellar Enhanced Ultrafiltration) (Nguyen et al., 2008).

In terms of environmental sustainability, biodegradability, removal efficiency, and eco-friendliness, Micellar Enhanced Ultrafiltration (MEUF) using sophorolipid has excellent potential. Furthermore, sophorolipids are more environmentally friendly, reusable, and sustainable than other nutrient removal technologies (Ghadge et al., 2015). Biodegradability, low toxicity, and good surface-active properties are all attributes of amphiphilic biosurfactants. MEUF with sophorolipid was chosen as the treatment technique for this research due to a lack of previous studies and sustainability concerns (Bade & Lee, 2011).

## Chapter 3. Materials and Methods

### 3.1 Materials

Sodium nitrate ( $\text{NaNO}_3$ ), potassium sulfate ( $\text{K}_2\text{HPO}_4$ ), and ammonium chloride ( $\text{NH}_4\text{Cl}$ ) are used as a source of nitrogen and phosphorus. These reagent salts were provided by Fisher Scientific Co. Nitric acid (66-70%) and sodium hydroxide ( $\text{NaOH}$ ) were purchased from Fisher Scientific Co. as an acid and base, respectively.  $\text{HNO}_3$  (0.5 N) and  $\text{NaOH}$  (0.5 N) were used to adjust the pH. The source of  $\text{NO}_3^-$  salt was derived from  $\text{NaNO}_3$ ,  $\text{PO}_4^{3-}$  salt was derived from  $\text{K}_2\text{HPO}_4$ , and  $\text{NH}_4^+$  salt was derived from  $\text{NH}_4\text{Cl}$ .

#### Sophorolipid

In this work, the sophorolipids (S.L.) biosurfactant was utilized. Ecover 41% sophorolipids (SL18), high lactonic S.L., were employed in this investigation. These sophorolipids were provided by Ecover Co., Belgium, and were used in this experiment (Table 3.2). It was composed of 30% acidic and 70% lactonic S.L. *Candida bombicola* was grown on a mixture of vegetable oil (rapeseed oil) and glucose to create these sophorolipids (Develter and Lauryssen, 2010; Arab, 2018).

**Table 3. 1 Lactonic sophorolipids SL18 (Ecover, Belgium 2014).**

Parameter	Value
Active matter	41%
Appearance	Dark-colored liquid solution
pH	$4.9 \pm 0.5$
Minimum surface tension	32-34 mN/m
Wetting capability	Low

## 3.2. Instruments

### 3.2.1 Ultrafiltration system

The QuixStand BenchTop System (Figures 3.1 and 3.2) (M series from A/G Technology Corporation) was used for the separation of nutrients ( $\text{NH}_4^+$ ,  $\text{PO}_4^{3-}$  and  $\text{NO}_3^-$ ), which was attached to the surface of micelle from the solution of chromium-rhamnolipid. The system included a feed reservoir, peristaltic recirculation pump, inlet pressure gauge, hollow fiber cartridge (Xampler cartridge), retentate outlet, outlet pressure gauge, sampling valve, and back pressure valve.

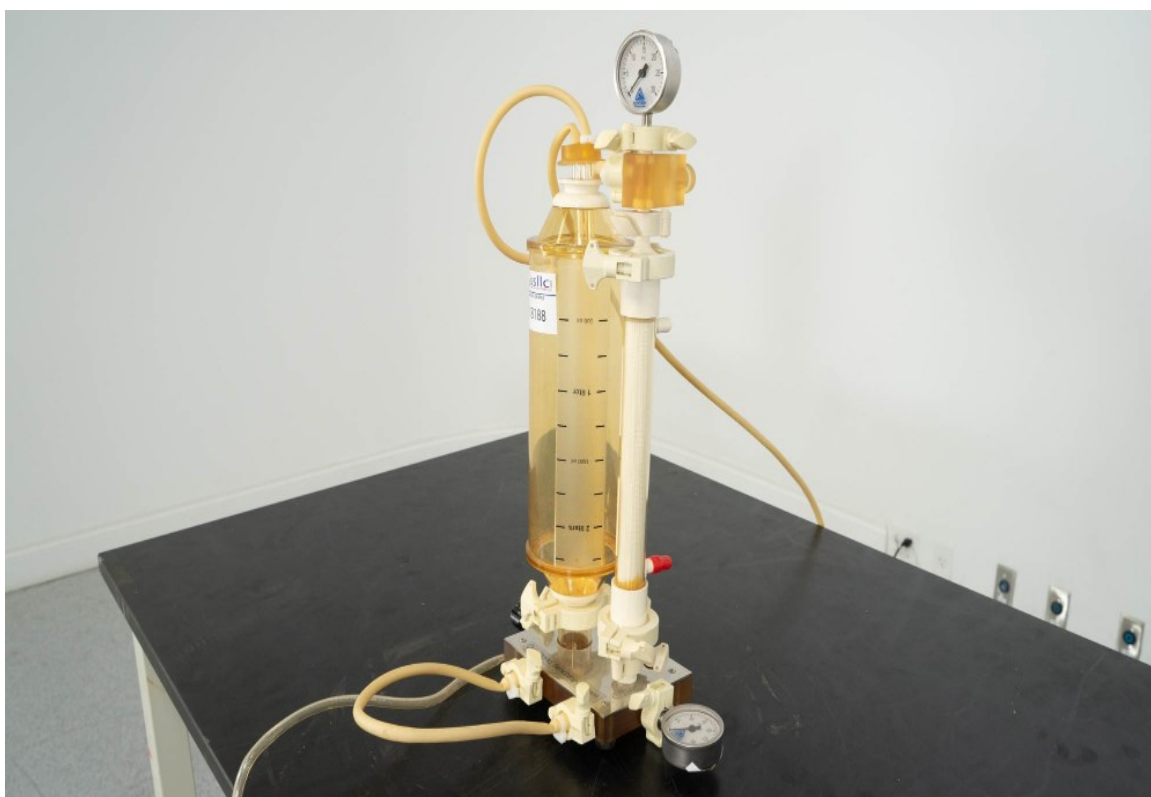


**Figure 3. 1 Ultrafiltration system with the reservoir (G.E Healthcare, 2004)**



**Figure 3. 2 QuixStand Benchtop System with a peristaltic pump (G.E Healthcare, 2004)**

### **3.2.2 Peristaltic pump**

The peristaltic pump that was included in the ultrafiltration system to pump the fluid was purchased from Watson-Marlow Company (313 S).

### **3.2.3 Xampler™ cartridge**

The hollow fiber cartridge used in QuixStand BenchTop (Ultrafiltration System) was purchased from A/G Technology Corporation. A bundle of polysulfone fibers parallels inside a plastic housing and forms the cartridge. Molecular Weight Cut-Off (MWCO) is essential in classifying ultrafiltration membranes. The MWCO that was used in the experiments was 10000 MWCO.

### 3.2.4 Miscellaneous instruments

Additional instruments used in this research are as follows.

Professional Sample Processor: The sample of synthetic wastewater containing  $\text{NH}_4^+$ ,  $\text{PO}_4^{3-}$ , and  $\text{NO}_3^-$  was placed in the sample processor to obtain the ion concentration. The results were acquired by executing MagIC Net's program on P.C. software. The software coordinates and analyzes the instrument and evaluates and manages the measured data in a database.



**Figure 3. 3 930 Compact I.C. Flex.**

Ion Chromatograph and Analysis: The 930 Compact I.C. Flex is a reliable ion chromatograph utilized in this experiment to detect reduction after membrane filtration (Figure 3.3). The pH was measured using the AR25 Dual Channel pH/Ion Meter from Fisher Scientific Co. In ICP-MS

analysis, the samples are introduced to high-temperature, argon-based plasma through pneumatic nebulization. By using ion chromatography (I.C.) and inductively coupled plasma mass spectrometry (ICP-MS) analyses, ions in the water were identified, respectively. For each analysis, 10 mL of samples were collected. The target elements dissolve and are ionized due to energy transference from the plasma to the sample stream. Using a mass spectrometer (quadrupole or magnetic), the resulting ions are separated from plasma-based on their mass-to-charge ratio. The separated ions are counted by an electron multiplier detector. The resulting information is processed by a computer. For this analysis, samples from untreated wastewater, MEUF permeate, were collected and diluted by the factor of 10, meaning 1 mL of sample was mixed with 9 mL of DI water.

Ion chromatography (I.C.) is a form of liquid chromatography which measures the concentration of ions based on their interaction with resin (stationary phase) and the eluent (mobile phase). There are an anion column and a cation column (each time only one of them) which attract anions and cations, respectively. Depending on their affinity for the specific resin, ion moves in the chromatographer column at different speeds, and they will be separated based on their size and ion charge. Then, the eluent passes through the column, and ions with weaker affinity to the column eluted faster and vice versa. A conductivity detector will measure the ions as they exit the column and plot conductivity vs. time. Each ion produces a peak on the graph, showing its concentration in the injected solution. In the tests, oxalic acid and sodium carbonate were the eluents for determining cations and anions, respectively. Samples from the untreated wastewater, U.F. permeate, and retentate was taken after each 2, 5, 10, and 20 min run and diluted by the factor of 10, meaning 1 mL of sample was mixed with 9 mL of DI water.

- The used shaker was AROS 160 adjustable reciprocating orbital shaker.
- The Tensiomat 21 was purchased from Fisher Scientific. The company was utilized to measure the apparent surface tension and interfacial tension of liquids.

- The traceable manometer gauge was purchased from the Control Company. The device can show gauge and differential pressure/vacuum in eleven units, and it has a response time of 0.5 seconds. The device has a simple hose fitting that allows hose/tubing with different inside diameters ranging from 1/16 to 3/16 centimeters.

### **3.3 CMC of Sophorolipid**

The surface tension of the surfactant at various concentrations is one of the primary methods for determining the biosurfactant' critical micelle concentration (CMC).

The surface tension of sophorolipids in various concentrations was measured using a tensiometer according to the Du Nouy method (Fisher Scientific, Tensiomat model 21). The force required to lift a thin metal ring (platinum ring) from the solution's surface is measured with a tensiometer (Mulligan et al., 2010). To assure the accuracy of the data, the tensiometer was first calibrated by measuring the surface tension of DI water. To measure the sophorolipid critical micelle concentration (CMC), the solution was diluted several times (Abbasi-Garravand & Mulligan, 2014). The surface tension of the solution was determined by submerging a platinum ring in the solution after each dilution step. The CMC of sophorolipid was determined using the Du Nouy method by plotting the surface tension versus biosurfactant concentration. The ring was inserted into the solution and then pulled out in the Du Nouy ring method. The sample mount was gradually lowered, stretching the liquid film formed beneath the ring until it splits and releases the ring. The surface tension was read directly in mN/m with the Tensiomat Model 21. Surface tension was then plotted against the sophorolipid concentration. The CMC of sophorolipid was calculated by drawing the intersection of two tangents on the graph. By examining the curve, it can be seen that increasing the concentration of sophorolipids lowers the surface tension until it reaches a

point where increasing the concentration of sophorolipids has no effect on the surface tension this point is known as the CMC (Mulligan et al., 2010; Arab, 2008).



**Figure 3. 4 Tensionmat 21 (Fisher Scientific).**

### **3.5 Ion Solution**

Dissolving 137.1 mg/l  $\text{NaNO}_3$ , 183.4 mg/L  $\text{K}_2\text{HPO}_4$ , and 296.5 mg/l  $\text{NH}_4\text{Cl}$  in 1 litre of double distilled water yielded a stock solution of 100 mg/L  $\text{NH}_4^+$ ,  $\text{PO}_4^{3-}$ , and  $\text{NO}_3^-$ . The decrease of  $\text{NH}_4^+$ ,  $\text{PO}_4^{3-}$  and  $\text{NO}_3^-$  by sophorolipid at varied pHs and sophorolipid concentrations was studied in batch studies. To achieve equilibrium, the prepared samples were agitated at 60 rpm for 24 hours, then centrifuged and analysed. Ion chromatography was used to determine the starting and final ion concentrations. The ion chromatograph is connected to a sample processor in this approach, which is always controlled by high-performance P.C. software like Metrohm's MagIC Net. The results were obtained by running MagIC Net's program on a P.C. The software

controls and analyses the instrument, as well as evaluates and managing the data collected in a database. The final percentage was determined by multiplying the concentrations obtained by the appropriate the dilution factor.

Equation 3.1 (Abbasi-Garravand & Mulligan, 2014) used to calculate the percentage anion and cation reduction was:

$$\% Ion_{reduction} = \frac{Ion\ Concentration_{initial} - Ion\ Concentration_{final}}{Ion\ Concentration_{initial}} * 100\% \quad \text{Equation 3.1}$$

### 3.6 Study of Transmembrane Pressure (TMP)

For observation of the effect of TMP on the permeate flux, various TMP (40, 50, 100, and 150 kPa) were chosen. This experiment was performed at 23°C and pH 6. The feed solution contained 0.3% sophorolipid. The permeate pressure was measured by a traceable manometer/pressure/vacuum gauge, and the TMP was determined based on the following equations (Abbasi-Garravand & Mulligan, 2014):

$$Transmembrane\ pressure = \frac{(P_{inlet} + P_{outlet})}{2} - P_{permeate} \quad \text{Equation 3.2}$$

The permeate flux was measured using this equation:

$$Flux \left( \frac{L}{m^2.h} \right) = \left\{ \frac{permeate\ flow \left( \frac{mL}{min} \right)}{cartridge\ area (m^2)} \right\} * .06 \quad \text{Equation 3.3}$$

The cartridge area was 140 cm<sup>2</sup>, and the permeate flow was measured by using the flowmeter for the permeate flow in the ultrafiltration system.

### 3.7 Effect of Different pH Values

Considering pH plays such a significant role in reducing NH<sub>4</sub><sup>+</sup>, PO<sub>4</sub><sup>3-</sup>, and NO<sub>3</sub><sup>-</sup> ions, the effect of varying pH levels was investigated. Because the pH of the solution after adding

sophorolipid is 7.82, the solutions were tested at pH 6, 7, 8, 9, and 10. Each test was conducted in triplicate, and the total sample amount was 50 mL. Temperature, anion, cation, and sophorolipid concentrations were fixed at 100 mg/L for  $\text{NH}_4^+$ ,  $\text{PO}_4^{3-}$ , and  $\text{NO}_3^-$ , respectively, and 0.3 % of sophorolipid. The pH was adjusted with 0.5 N NaOH and 0.5 N  $\text{HNO}_3$ , and the initial and final contents of  $\text{NH}_4^+$ ,  $\text{PO}_4^{3-}$ , and  $\text{NO}_3^-$  were determined using ion chromatography.

### **3.8 Effect of Sophorolipid Concentration**

To assess the impact of sophorolipid concentration on the decrease of  $\text{NH}_4^+$ ,  $\text{PO}_4^{3-}$  and  $\text{NO}_3^-$  ions, different percentages of sophorolipid (0.01%, 0.02%, 0.03%, 0.1%, 0.2%, 0.3%, 0.4%, 0.5%, 1%, 2%) were prepared. Each sample had a pH of 6 with 100 mg/L of  $\text{NH}_4^+$ ,  $\text{PO}_4^{3-}$ , and  $\text{NO}_3^-$ . These samples had a total volume of 50 ml.  $\text{HNO}_3$  (0.5 N) and NaOH (0.5N) were used to alter the pH. Each test was repeated three times, and the average was displayed as the final result. The optimal sophorolipid concentration was the one that resulted in the highest  $\text{NH}_4^+$ ,  $\text{PO}_4^{3-}$ , and  $\text{NO}_3^-$  ions decrease.

### **3.9 Effect of Anion and Cation Concentration**

Under identical conditions (sophorolipid concentration=0.3%, pH 6, and  $T = 22^\circ\text{C}$ ), various amounts of anions were tested and studied to determine the optimal removal of  $\text{PO}_4^{3-}$  and  $\text{NO}_3^-$  at concentrations of  $\text{NO}_3^-$  (25, 50, 100 and 200 mg/L) and  $\text{PO}_4^{3-}$  (25, 50, 100, and 200 mg/L) respectively. For each concentration, three solutions were tested. Following the addition of the sophorolipid, the pH was adjusted using 0.5 N NaOH and 0.5 N  $\text{HNO}_3$ . The

volume of each sample was 50 mL. After 24 hours of shaking, the final ion concentration was determined using ion chromatography to determine the concentration of  $\text{PO}_4^{3-}$  and  $\text{NO}_3^-$ .

Different concentrations of cations were tested and analyzed under identical conditions (sophorolipid concentration=0.3%, pH 6, and  $T = 22^\circ\text{C}$ ) to identify the largest removal of  $\text{NH}_4^+$ , at various concentrations of ammonium ( $\text{NH}_4^+$ ) (25, 50, 100, and 200 mg/L) ( $\text{NH}_4^+$ ). Three samples were produced for each concentration. The pH was then adjusted with 0.5 N NaOH and 0.5 N  $\text{HNO}_3$  after adding a sophorolipid. All samples had a volume of 50 mL. After shaking all the samples for 24 hours, the final ion concentration was evaluated using ion chromatography to determine the concentration of  $\text{NH}_4^+$ .

### **3.10 Effect of Temperature**

The influence of temperature on removal rate was examined in this experiment by utilizing varied feed solution temperatures (25, 30, 35, 40, and  $45^\circ\text{C}$ ). Room temperature, transmembrane pressure, and pH were kept constant, and the solution had a pH of 6 and included 100 mg/L of  $\text{NH}_4^+$ ,  $\text{PO}_4^{3-}$ , and  $\text{NO}_3^-$  and 0.3 % sophorolipid. Ion chromatography was used to determine the ion concentrations.

### **3.11 Membrane Unit Experiments**

These tests were carried out in batches. The feed solution had a volume of 400 mL at the beginning, and the retentate stream was continually recycled. The water flux was monitored before and after the experiment at the optimal transmembrane pressure to confirm membrane fouling. It was time to clean the membrane when the water flux was less than 80-

90% percent of the flux of a new membrane. The procedure will be described in the section on ultrafiltration system cleaning.

The sodium nitrate, dipotassium hydrogen phosphate, and ammonium chloride salts were dissolved in distilled water to make a stock solution of  $\text{NH}_4^+$ ,  $\text{PO}_4^{3-}$  and  $\text{NO}_3^-$ , and required concentrations of  $\text{NH}_4^+$ ,  $\text{PO}_4^{3-}$  and  $\text{NO}_3^-$  were made by diluting the stock solution with the same water. Distilled water was used to dilute Ecover sophorolipids (41%) (SL18) to make various molar solutions of sophorolipids. The reservoir's feed solution, which contained anions, cations, and sophorolipid, was fed through the ultrafiltration membrane by a peristaltic pump. The retentate solution was returned to the feed reservoir after exiting the cartridge. Ion Chromatography was used to measure the concentrations of  $\text{NH}_4^+$ ,  $\text{PO}_4^{3-}$ , and  $\text{NO}_3^-$  in the permeate, retentate, and feed samples. All tests were conducted at a temperature of 22°C and a pH of 6. After each experiment, the flow loop was cleansed by running distilled water through the apparatus. Each test was done three times, and the average was used to determine the outcome.

### **3.12 Cleaning the Ultrafiltration Membrane**

The ultrafiltration system was cleaned in seven phases. The retentate should be drawn out first. The system was then cleansed with double distilled water. In the third phase, 0.5 N NaOH was recirculated for one hour. The system should then be cleansed a second time using double distilled water. In the fifth phase, NaOCl was recirculated through the system for one hour and at pH 10-11, and the system was flushed with double distilled water for the last time. Finally, the collected sample from the permeate was examined for residual anions and cations.

## **Chapter 4: Results and Discussion**

### **4.1 CMC Determination**

The critical micelle concentration (CMC) of the sophorolipids utilized in this investigation was determined to be 30 mg/L or 0.003% of the sophorolipid. By determining the CMC of the biosurfactants, the minimum concentration that micelles would be formed and the lowest concentration for the optimum performance of biosurfactant solution is determined. Furthermore, by measuring the CMC of the effluent from the experiment, biosurfactant concentration in the effluent can be determined, and the correlation of biosurfactant adsorption to the media to biosurfactant concentration can be determined.

There is a considerable difference between the values of the CMC of different types of biosurfactants. The lower the CMC value is, the less biosurfactant is a need. The cost of biosurfactants is a significant portion of the remediation cost, corresponding to the quantity of the biosurfactant used. Therefore, a biosurfactant's desirable property is having a low critical micelle concentration (CMC) (Mulligan, 2005).

The surface tension was found to be 44 mN/m at that concentration. This CMC was calculated by finding the intersection of two tangent lines in Figure 4.1, as discussed in the previous chapter. The surface tension is dependent on the sophorolipid content, as seen in Figure 4.1. The surface tension drops from 72.5 to 44 mN/m when the concentration of Sophorolipid rises from 0 to 30 mg/L. This dramatic decrease in surface tension is caused only by the very little increase in sophorolipid concentration. This tendency continues as sophorolipid

concentration rises from 30 mg/L to 1000 mg/L, although the surface tension decreases gradually from 44 to 37 mN/m (Mulligan et al., 2010) (Chen et al., 2020).

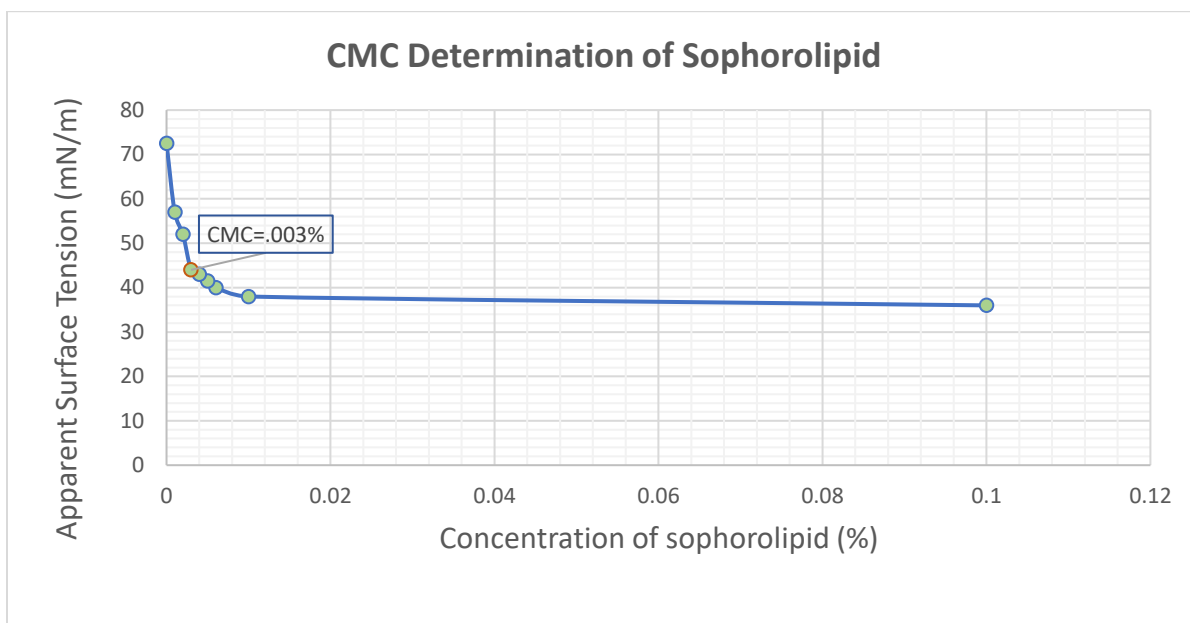


**Figure 4. 1 CMC Determination of Sophorolipid.**

In the experiments, SL concentration was chosen to be higher than CMC for increasing the biosurfactant to pollutant ion ratio and better removal.

## 4.2 Significance of CMC Value

The critical micelle concentration (CMC) of a biosurfactant is the intercept of two straight lines from the concentration-dependent and concentration-independent sections of the graph of surface tension vs. logarithmic biosurfactant concentration (Yenphan et al., 2010). Although this method is one of the easiest ways of measuring the quality of a biosurfactant, it should be noted that the presence of other components in the solution can cause errors in the results. Moreover, it should be pointed out that the CMC should be considered as a range of concentrations and not a point, as by changing the concentration, the size of the aggregate changes and affects the CMC value (Chen et al., 2020)

According to Wang and Mulligan (2009b), the efficiencies of biosurfactants in removing contaminants increase linearly as the surfactant concentration increases until it reaches the CMC concentration. Beyond the CMC point, the effectiveness of biosurfactants remains moderately constant. The researchers above recommended using higher concentrations than the CMC concentration to overcome the effects of surfactant sorption by the contaminant particle (Puasa et al., 2011). Initially, an SL concentration of 0.03% was chosen in this proposed study, and the removal rate was not satisfactory (Chen et al., 2020). A higher removal rate was achieved by increasing the SL concentration to 0.3% and lowering the ion concentration in the synthetic solution (Silva et al., 2010). The other factors influencing the CMC are the presence of congeners and homologs of the biosurfactant in the solution. As homologs and congeners have their CMC value, the CMC of the mixture depends on the ratio of each one. When biosurfactants are not homogenized thoroughly, the sample taken from the solution after dilution may not retain the original ratios of congeners and homologs. Therefore the obtained CMC value cannot precisely determine the CMC value of the original sample (Kim et al., 2004).

The tests were carried out at the critical micelle concentration (CMC) and a higher SL concentration. A greater concentration of SL was added since the more micelles in the solution, the more influential the solution was (Moreno et al., 2022). Anionic contaminants such as nitrate and phosphate can be electrostatically bonded on the micelles, and the micelle-pollutant complex is successfully removed by ultrafiltration. Because ammonia has a positive charge, the elimination rate is higher in an alkaline condition (Samper et al., 2009).

#### **4.2.1 Effects of different parameters in pollutant ion removal**

In this section, the effect of variation in parameters such as pH, temperature, SL concentration, and initial ion concentration will be discussed. Micellar enhanced ultrafiltration has been chosen for the removal of the ions from the synthetic solution containing  $\text{NO}_3^-$ ,  $\text{PO}_4^{3-}$ , and  $\text{NH}_4^+$  ions. Sophorolipid is supplied to the aqueous stream at a concentration (0.03% and 0.3%, respectively) higher than their critical micelle concentrations in this process. In this study, there were two different tests conducted, one with a pollutant ion to sophorolipid ratio of 1:1.3 (mol/mol) (Ions: SL=1:1.3) and the second was 13.5:1 (mol/mol) (Ions: SL=13.5:1). Addition of sophorolipid to the synthetic solution with ions forms micelle larger than the pore size of the ultrafiltration membrane. This micelle solution is subsequently filtered via an ultrafiltration membrane with a molecular weight cut-off (MWCO) size of 10000 in this experiment (Abbasi-Garravand & Mulligan, 2014).

#### **4.3 Effect of pH on Removal Rate (Ions: SL=1:1.3)**

This part of Chapter 4 will discuss the effect of a variable pH range on ion removal ( $\text{NO}_3^-$ ,  $\text{PO}_4^{3-}$ , and  $\text{NH}_4^+$ ). The removal rate varies based on the property of ions and the overall pH of the solution. The range of pH chosen for this test was from pH 6 to 10. At the lower pH, the removal rate of nutrient ions is higher and vice-versa. In the solution, there are two anions and one cation. So the impact of pH on the removal rate can be explained by anion exchange and reduction of the anions in the solution ( $\text{NO}_3^-$ ,  $\text{PO}_4^{3-}$ ) (El Zeftawy & Mulligan, 2011).

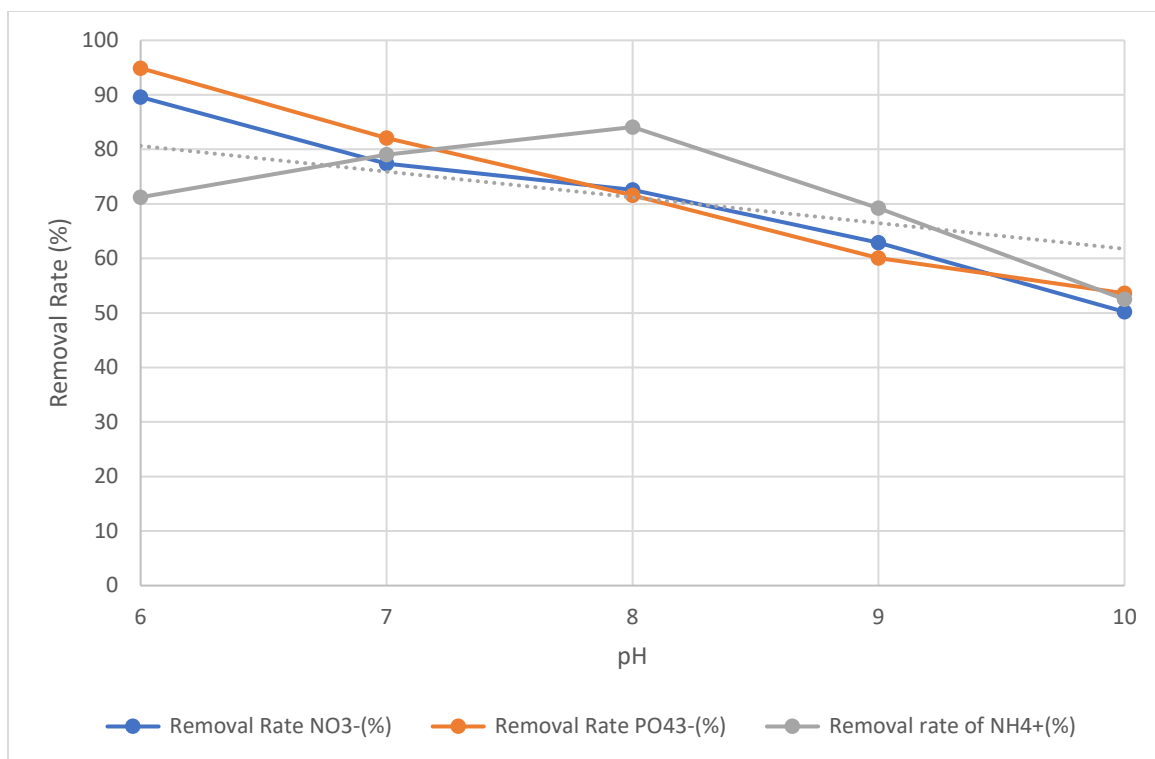


**Figure 4. 2 Effect of pH on removal rate of NO<sub>3</sub><sup>-</sup>, PO<sub>4</sub><sup>3-</sup> and NH<sub>4</sub><sup>+</sup>, SL concentration= 0.3%, temperature=22°C, NO<sub>3</sub><sup>-</sup>, PO<sub>4</sub><sup>3-</sup> and NH<sub>4</sub><sup>+</sup> concentration=100 mg/l, molecular weight cut-off (MWCO)=10,000, TMP= 120 kPa, flow rate =70 rpm**

#### **4.4 Effect of pH on Removal Rate(Ions:SL=13.5:1)**

This section shows the relation between pH changes and ion removal rate in Fig 4.3 using a lower SL concentration and a higher pollutant ion concentration. The pH varied from 6 to 10. The removal rate was lower compared to the previous test due to a higher ion to sophorolipid ratio.

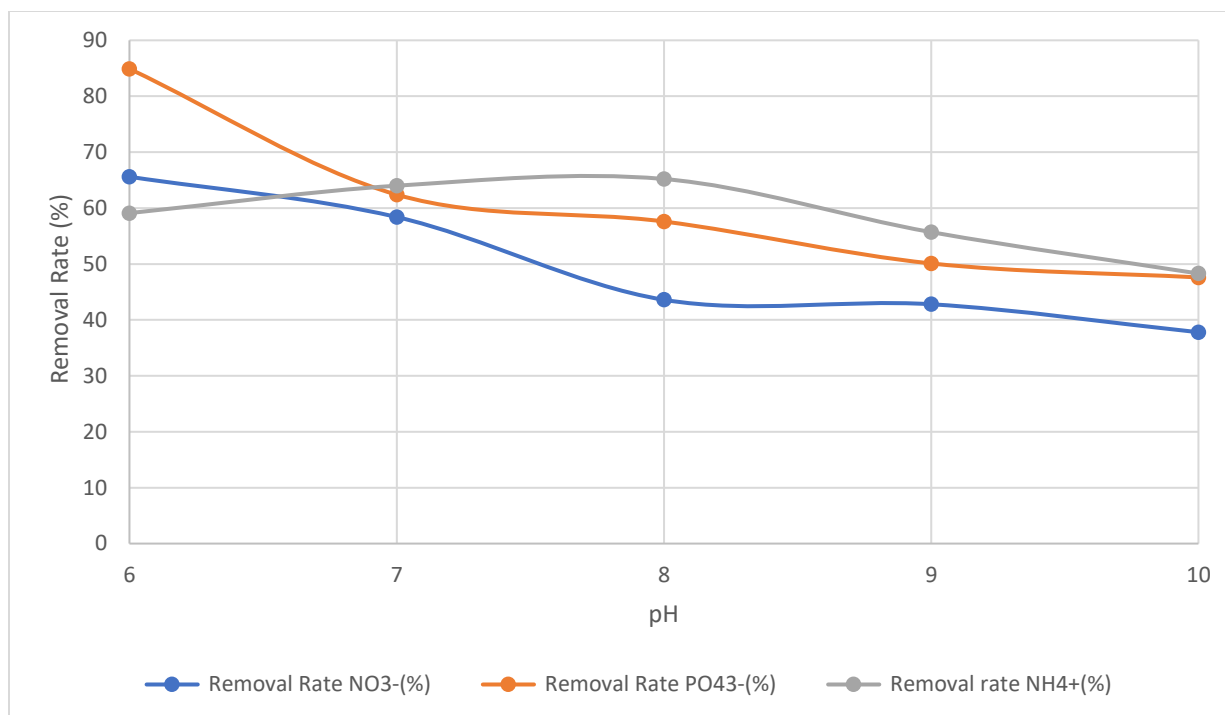


**Figure 4. 3 Effect of pH on removal rate of  $\text{NH}_4^+$ ,  $\text{NO}_3^-$ ,  $\text{PO}_4^{3-}$ , concentration of  $\text{NH}_4^+$  =575 mg/L, concentration of  $\text{PO}_4^{3-}$ =818.9 mg/L and concentration of  $\text{NO}_3^-$  is 2042 mg/L SL concentration=0.03% and the temperature=22°C. The molecular weight cut-off (MWCO)=10,000.**

According to Baccile et al. (2012), acidic sophorolipids are sensitive to pH, temperature, and electrical fields. This can result in changes in their efficiency. By altering the pH level, different aggregate states of sophorolipids can be obtained (Baccile et al., 2013). Daverey and Pakshirajan (2009) investigations showed that changing the pH affected the performance of sophorolipids. At neutral pH levels, sophorolipids show high emulsifying activity. However, with decreasing pH decrease, the stability of the emulsion formed (Yaquab & Lee, 2019).

#### 4.5 Effect of Temperature on Permeate Flux (Ions: SL=1:1.3)

The effect of temperature on flow was studied in this experiment throughout a temperature range of 22°C to 45°C. Other parameters were all kept constant. When the temperature rises, the flux also increases, as seen in Figure 4.4. Although the temperature on permeate flow is not as large as the effect of transmembrane pressure, the pattern is similar.

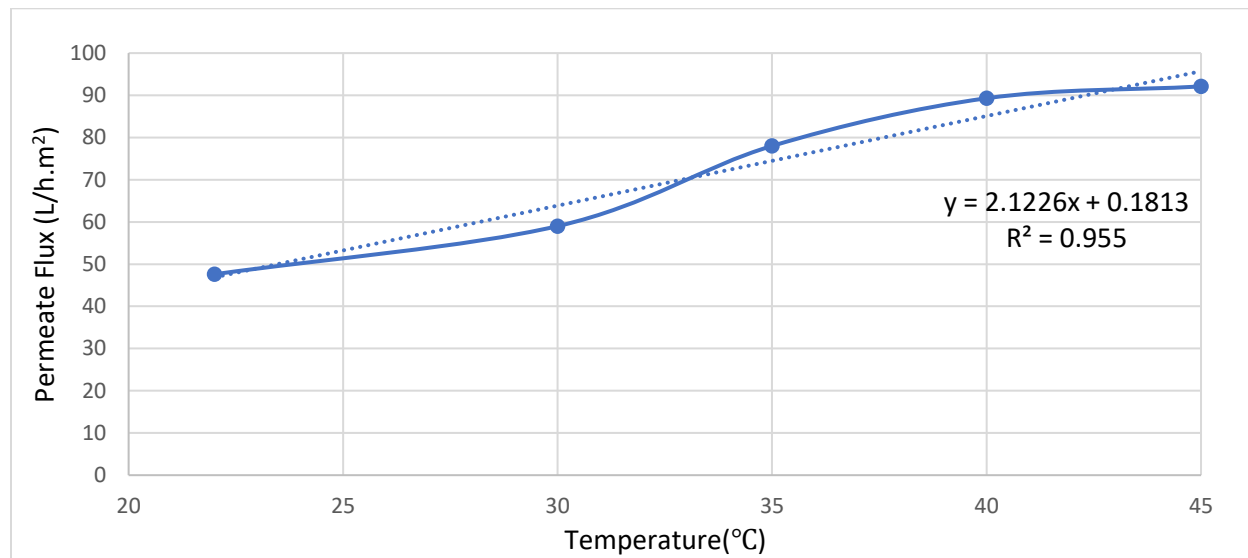


**Figure 4. 4 Effect of temperature on permeate flux at pH 6,  $\text{NH}_4^+$ ,  $\text{NO}_3^-$ ,  $\text{PO}_4^{3-}$  = 100 mg/L  
SL concentration= 0.3%, temperature=22°C, molecular weight cut-off (MWCO)=10,000,  
TMP= 120 kPa, flow rate =70 rpm**

The viscosity of the synthetic solution containing the sophorolipid solution decreases as the temperature rises, causing the flux to rise. The flux reached a high of 92.1 L/h.m<sup>2</sup> at 45°C and a low of 47.6 L at 20°C.

#### 4.6 Effect of temperature in Permeate Flux (Ions: SL=13.5:1)

The effect of temperature on flow was studied in this experiment throughout a temperature range of 22°C to 45°C. The pH, initial sophorolipid concentration, transmembrane

pressure, and sophorolipid concentration were all kept constant. When the temperature rises, the flux increases with it, as seen in Figure 4.5.

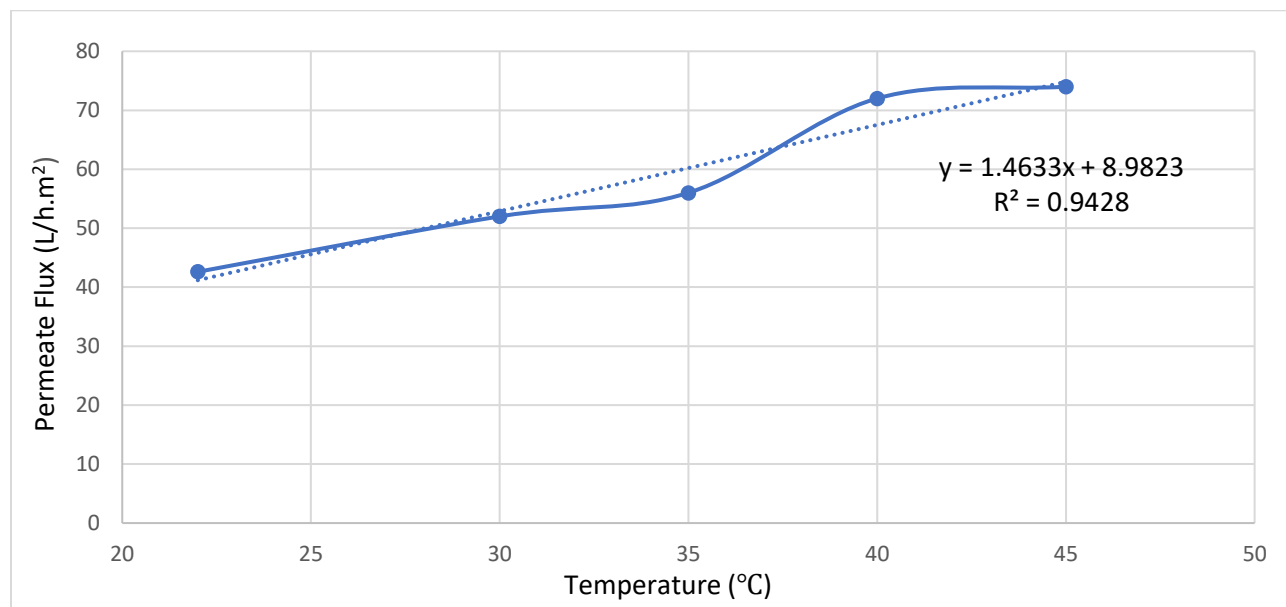


**Figure 4. 5 Effect of Temperature on Permeate Flux at pH 6, concentration of  $\text{NH}_4^+$  =575 mg/L, concentration of  $\text{PO}_4^{3-}$ =818.9 mg/L and concentration of  $\text{NO}_3^-$  is 2042 mg/L SL concentration=0.03% and the temperature=22°C. The molecular weight cut-off (MWCO)=10,000.**

#### **4.7 Effect of Temperature on Removal Rate (Ions: SL=1:1.3)**

The relation between temperature change and the ion removal ( $\text{NO}_3^-$ ,  $\text{PO}_4^{3-}$  and  $\text{NH}_4^+$ ) was evaluated. The temperature varied from 25°C to 45°C. Figure 4.6 shows that the highest removal rate of  $\text{NO}_3^-$  was 96.9% at a temperature of 45°C, and the lowest was 69.1% at a temperature of 25°C. The permeate flow increases as the temperature rise due to the membrane material's thermal expansion and lower solution viscosity (Ghadge et al., 2015). Because the surfactant

CMC varies with temperature, the temperature is the most significant parameter for MEUF (Batista et al., 2006).

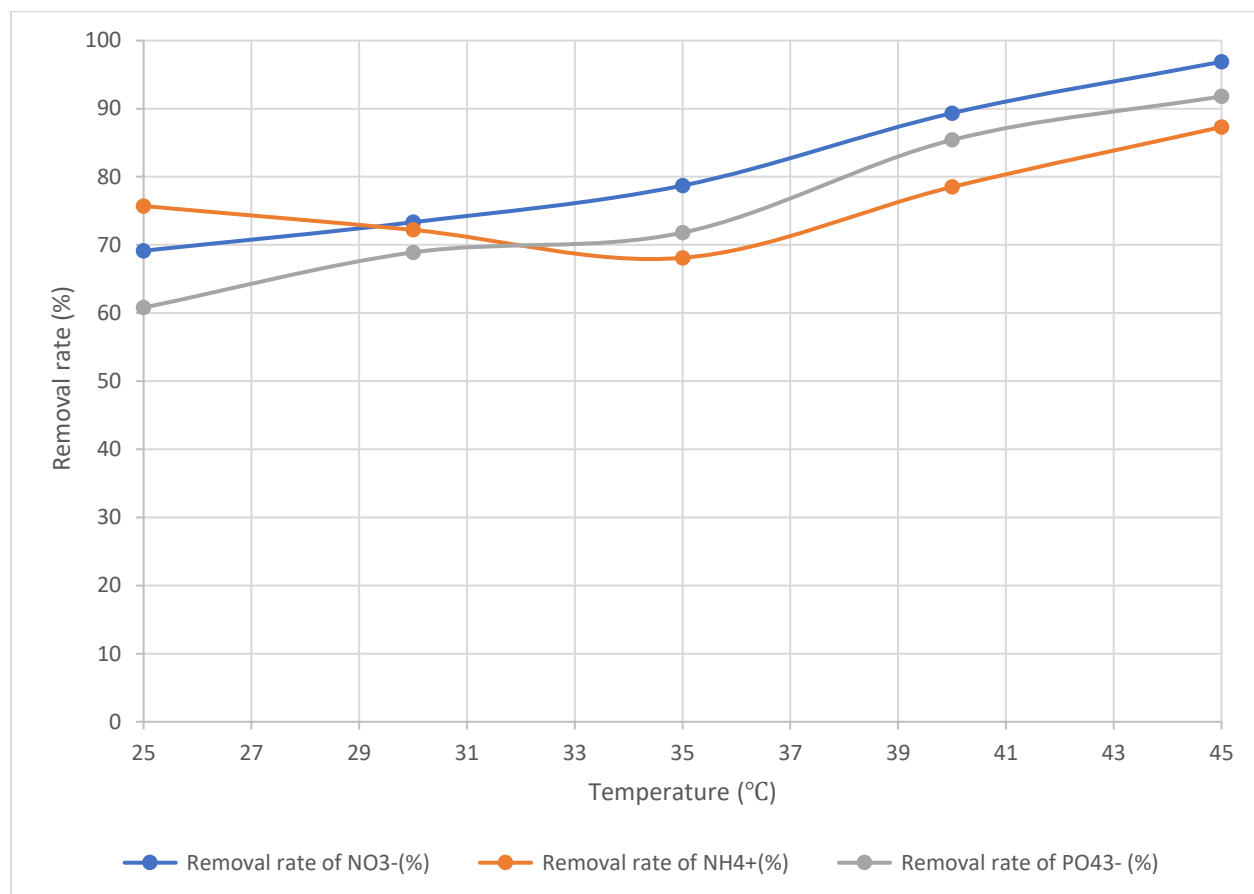


**Figure 4. 6 Effect of temperature on removal rate of NO<sub>3</sub><sup>-</sup>, PO<sub>4</sub><sup>3-</sup> and NH<sub>4</sub><sup>+</sup>, concentration of NO<sub>3</sub><sup>-</sup>, PO<sub>4</sub><sup>3-</sup> and NH<sub>4</sub><sup>+</sup> = 100 mg/L SL concentration= 0.3%, temperature=22°C, molecular weight cut-off (MWCO)=10,000, TMP= 120 kPa, flow rate =70 rpm**

#### **4.8 Effect of Temperature on Removal Rate (Ions: SL=13.5:1)**

This section shows the relation between temperature change and ion removal (NO<sub>3</sub><sup>-</sup>, PO<sub>4</sub><sup>3-</sup>, and NH<sub>4</sub><sup>+</sup>). The variable temperature was selected to measure the removal rate of NO<sub>3</sub><sup>-</sup>, PO<sub>4</sub><sup>3-</sup>, and

$\text{NH}_4^+$ . As  $\text{NH}_4^+$  is volatile, the sudden drop in the removal rate at 35°C can be explained (Silva et al., 2010).

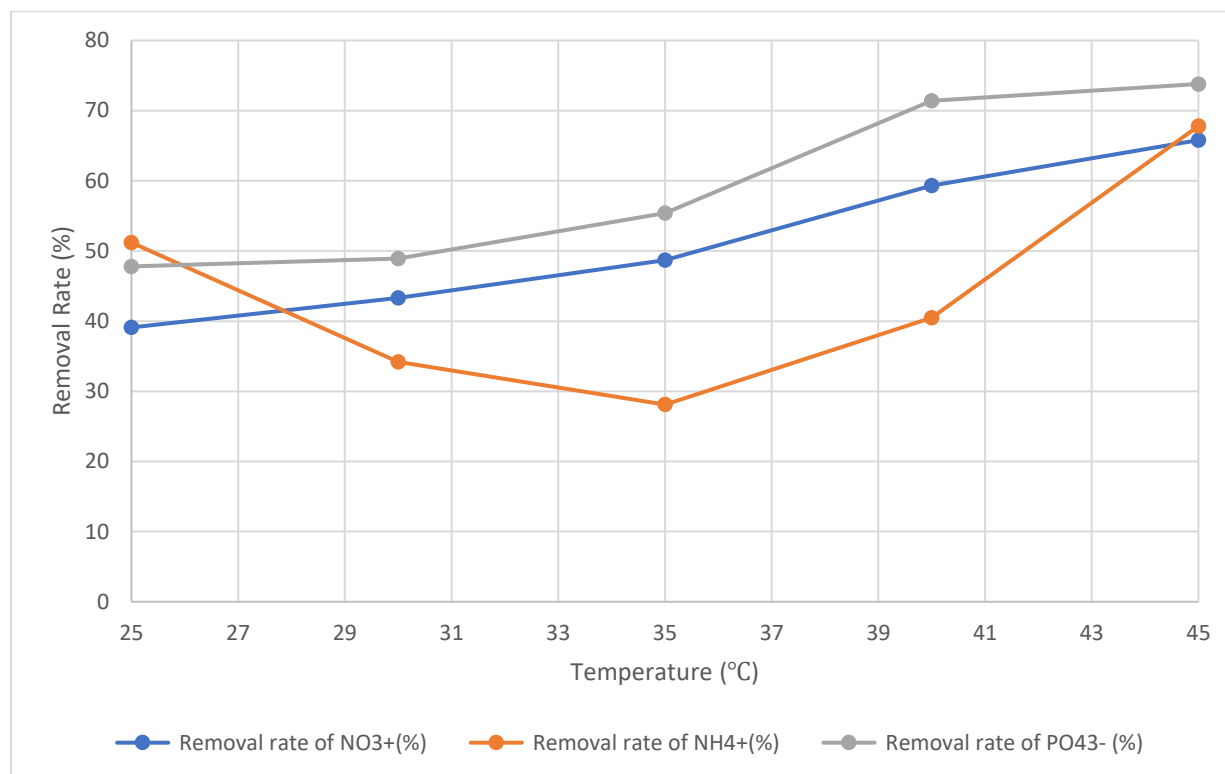


**Figure 4. 7 Effect of temperature on removal rate of  $\text{NO}_3^-$ ,  $\text{PO}_4^{3-}$  and  $\text{NH}_4^+$ . The initial concentration of  $\text{NH}_4^+$ =575 mg/L,  $\text{PO}_4^{3-}$ =818.96 mg/L and  $\text{NO}_3^-$ =2042 mg/L, SL concentration=0.03%. Temperature=22°C, pH=6, membrane's molecular weight cut-off (MWCO)=10,000, TMP=120 kPa**

#### **4.9 Effect of Initial Concentration on Removal Rate (Ions: SL=1:1.3)**

The relation between the change of initial ion concentration of  $\text{NO}_3^-$ ,  $\text{PO}_4^{3-}$  and  $\text{NH}_4^+$  and the effect on the change of removal rate is shown in Fig 4.8. In this experiment, the removal rate of

$\text{PO}_4^{3-}$ ,  $\text{NH}_4^+$  and  $\text{NO}_3^-$  at various concentrations of initial nitrate ( $\text{NO}_3^-$ ), phosphate ( $\text{PO}_4^{3-}$ ), and ammonia ( $\text{NH}_4^+$ ) (25, 50, 100, 200 mg/L) was evaluated.

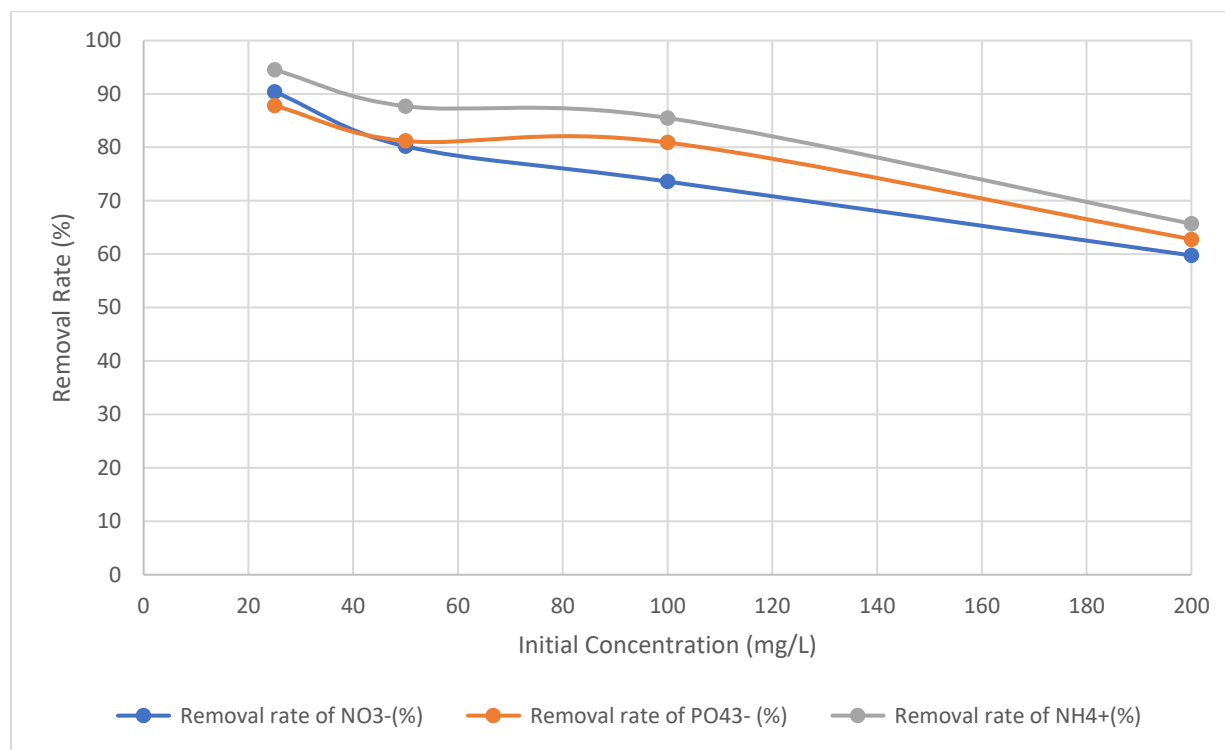


**Figure 4. 8 Effect of initial concentration on removal rate of  $\text{NO}_3^-$ ,  $\text{PO}_4^{3-}$  and  $\text{NH}_4^+$ , TMP=120 kPa, temperature=22°C and the sophorolipid concentration= 0.3%. The pH was 6, molecular weight cut-off (MWCO)= 10,000. The flow rate = 70 rpm**

As the initial ion concentration in the solution increases, the pollutant ion to sophorolipid concentration changes from 1:1.3 to 1: 0.8, As a result, the sites for attachment for nutrient ions are decreased, causing a lower removal rate (Vibhandik & Marathe, 2014).

#### **4.10 Effect of Initial Concentration on Removal Rate(Ions: SL=13.5:1)**

In this part, the relation between the initial ion concentration of  $\text{NO}_3^-$ ,  $\text{PO}_4^{3-}$  and  $\text{NH}_4^+$  and the effect on the removal rate is discussed. In this experiment, the removal rate of  $\text{PO}_4^{3-}$ ,  $\text{NH}_4^+$  and,  $\text{NO}_3^-$  at various concentrations of initial nitrate (510.5, 1021, 2042, and 4048 mg/L),

phosphate (204.7, 409.4, 818.9, and 1637.9 mg/L) and ammonium ( $\text{NH}_4^+$ ) (204.7, 409.4, 818.9, and 1637.9 mg/L) was evaluated. In Fig. 4.9, the highest removal rate of  $\text{NO}_3^-$  was 76.8% at an initial concentration of 510.5 mg/L, and the lowest was 24.6% at 4048 mg/L. The removal rates decreased owing to the increase of ion concentration to sophorolipid concentration. In this case, the ion concentration was doubled, owing to a lower removal rate.

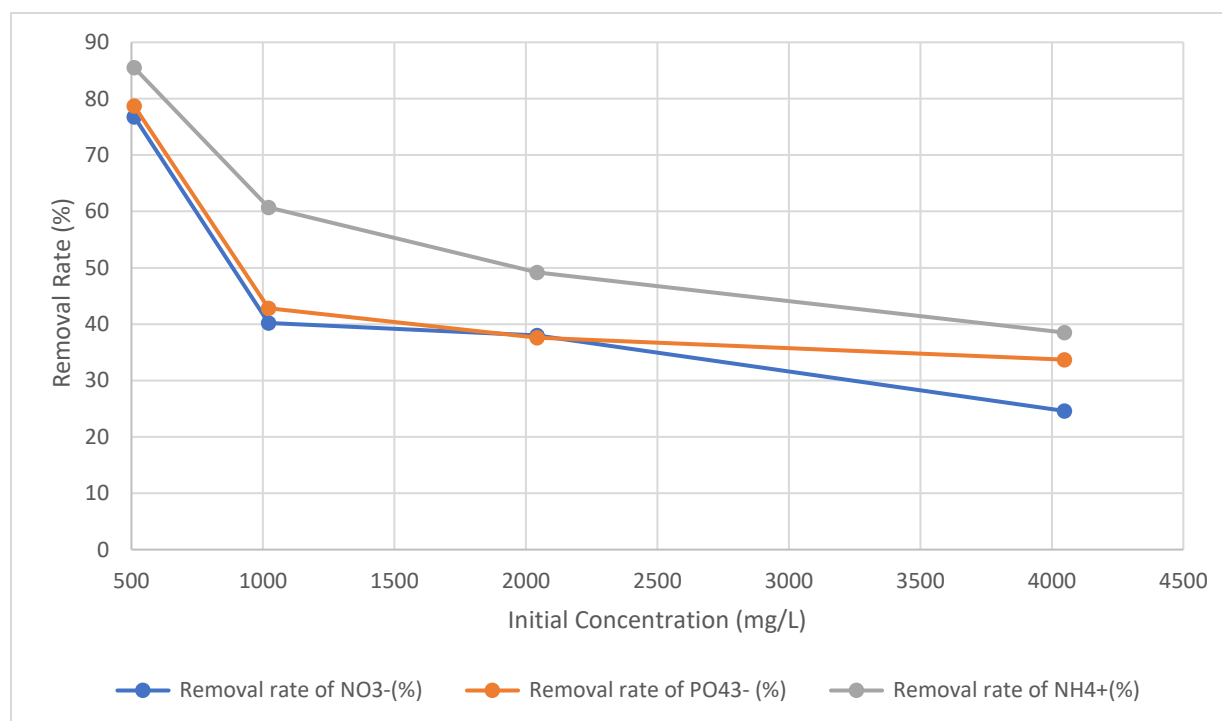


**Figure 4. 9 Effect of initial concentration on removal rate of  $\text{NO}_3^-$  ,  $\text{PO}_4^{3-}$  and  $\text{NH}_4^+$  at temperature= 22°C, sophorolipid concentration=0.03%, pH6, MWCO=10,000, TMP=120kPa**

#### 4.11 Effect of Sophorolipid Concentration on Removal Rate (Ions: SL=1:1.3)

This section showed how the removal rate varies with the variable concentration of sophorolipid in the solution. The sophorolipid concentration during this experiment was evaluated at 0.1%, 0.2%, 0.3%, 0.4%, 0.5%, 1% and 2% to determine the ion removal rate of  $\text{NO}_3^-$ ,  $\text{PO}_4^{3-}$  and  $\text{NH}_4^+$ . The highest removal rate of  $\text{NH}_4^+$  in Fig. 4.10 was 88.8% at 0.4%, and the lowest was 58.7% at 0.1% sophorolipid. This demonstrates that the removal rate of nutrient ions is proportional to sophorolipid content. This suggests that raising the concentration of SL from 0.1 mg/L to 0.3 mg/L (0.025–0.1 percent) promotes nutrient removal. When the concentration of SL in the feed solution rises, so does the concentration of micelles in the solution. This improves micelle clearance of nutrient ions.

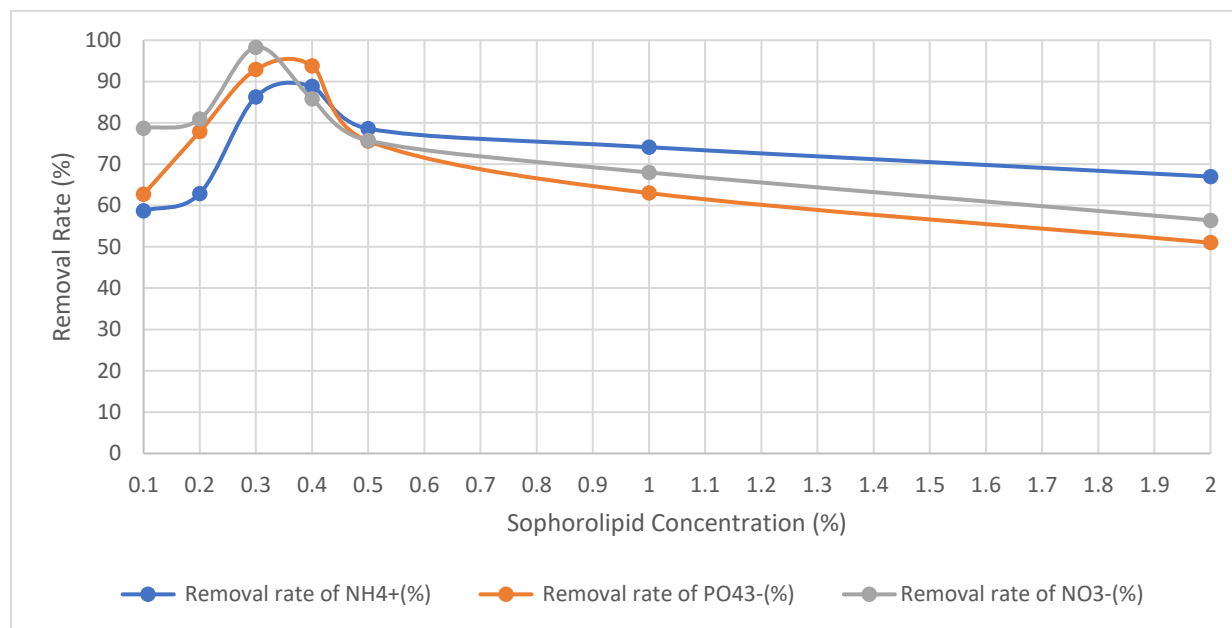


**Figure 4. 10 Effect of sophorolipid on removal rate of  $\text{NO}_3^-$ ,  $\text{PO}_4^{3-}$  and  $\text{NH}_4^+$ , at ion concentration=100 mg/L and TMP=120kPa, temperature=22°C and the sophorolipid concentration= 0.3%. The pH was 6, molecular weight cut-off (MWCO)=10,000, the flow rate = 70 rpm**

In Fig. 4.10, the highest removal rate showed the same trend where was 98.9% of  $\text{NO}_3^-$  was removed at 0.4% sophorolipid concentration and the lowest at a concentration of 2% sophorolipid concentration. The highest removal rate was observed at pollutant ion to sophorolipid concentration of 1:1.4. The greater removal rate at higher concentration can be explained as the more availability for attachment for the pollutant ion with the increased biosurfactant to pollutant ion ratio. Beyond that point, the fouling starts owing to less room for attachment for the ions and higher viscosity. After a particular sophorolipid concentration, the removal rate gets lowered again due to fouling and the higher viscosity of the solution (Moreno et al., 2022). In this particular case, the removal rate is decreased when the concentration is increased from 0.4%.

#### **4.12 Relation Between Surface Tension and Concentration of the Solution**

The apparent tension between the feed solution and the permeate was measured in order to verify the sophorolipid content of the solution both before and after the test using a tensiometer. The sophorolipid concentration is initially higher, but as a result of the recirculation process, the Sophorolipid is used up to create micelles, increasing the surface tension (Fig 4.11).

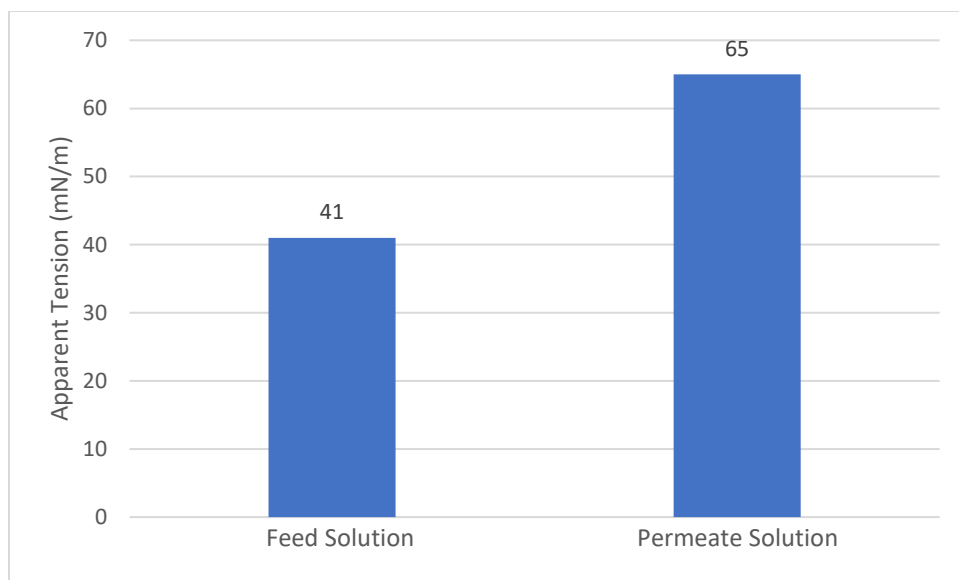


**Figure 4.11 Change of surface tension in the feed and permeate solution, ion concentration=100 mg/L, sophorolipid concentration=0.4%, temperature=22°C, pH=6, MWCO=10000, TMP=120kPa, the flow rate=70 rpm**

The apparent surface tension of the solution was measured before and after the filtering. The feed solution displayed reduced surface tension due to the addition of SL. The surface tension of the permeate solution increased after filtration, approximating the surface tension of pure water (72 mN/m), as SL in micelle form was rejected by the membrane, and only a few monomers passed through the membrane.

#### **4.13 Effect of Sophorolipid Concentration on Removal Rate (Ions: SL=13.5:1)**

In Fig 4.12, the highest removal rate of  $\text{NO}_3^-$  was 57.9% at 0.3%, and the lowest was 21.3% of 2% sophorolipid. It is demonstrated in Fig 4.12 that the highest removal rate  $\text{NH}_4^+$  was 57.9% at 0.3%, and the lowest was 21.2% for 2% sophorolipid. The same trends were shown for

phosphate and nitrate removal. The highest removal rate was observed at the sophorolipid to pollutant ion ratio of 1:13.

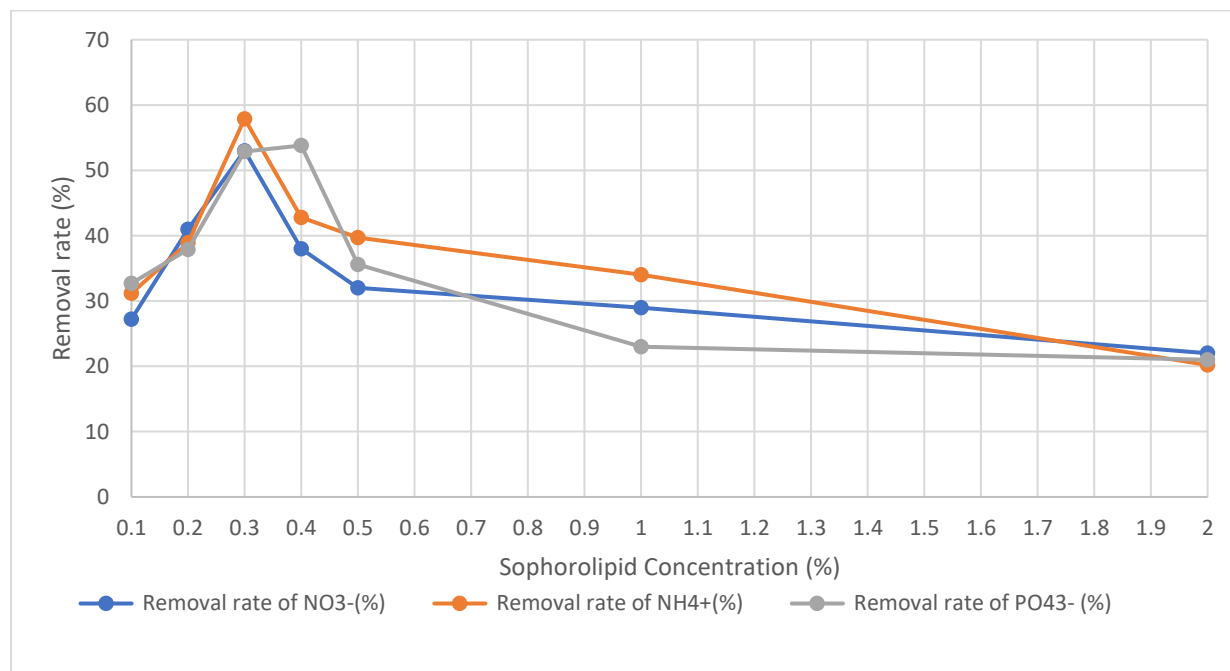


**Figure 4. 12 Effect of sophorolipid concentration on removal rate of  $\text{PO}_4^{3-}$ ,  $\text{NO}_3^-$  and,  $\text{NH}_4^+$ , The initial concentration of  $\text{NH}_4^+$  =575 mg/L,  $\text{PO}_4^{3-}$ =818.96 mg/L and  $\text{NO}_3^-$ =2042 mg/L. Temperature=22°C, pH=6, Molecular weight cut-off (MWCO) was 10,000. The flow rate= 70 rpm**

The greater removal rate at higher concentration can be explained as the more availability for attachment for the pollutant ion with the increased biosurfactant to pollutant ion ratio. Beyond that point, the fouling starts due to sorption on the membrane and higher viscosity. The removal rate is reduced once again after reaching a specific sophorolipid concentration due to

fouling and the solution's increased viscosity. In this scenario, as the concentration is raised 0.3 % to higher, the removal rate dropped for  $\text{NO}_3^-$  and  $\text{NH}_4^+$  (Verma & Sarkar, 2018).

#### 4.14 Effect of Transmembrane Pressure in Permeate Flux(Ions: SL=1:1.3)

As shown in Figure 4.13, increasing the transmembrane pressure (TMP) positively influences permeate flow, implying that as the TMP increases, the driving force starts to rise, resulting in the higher flux.

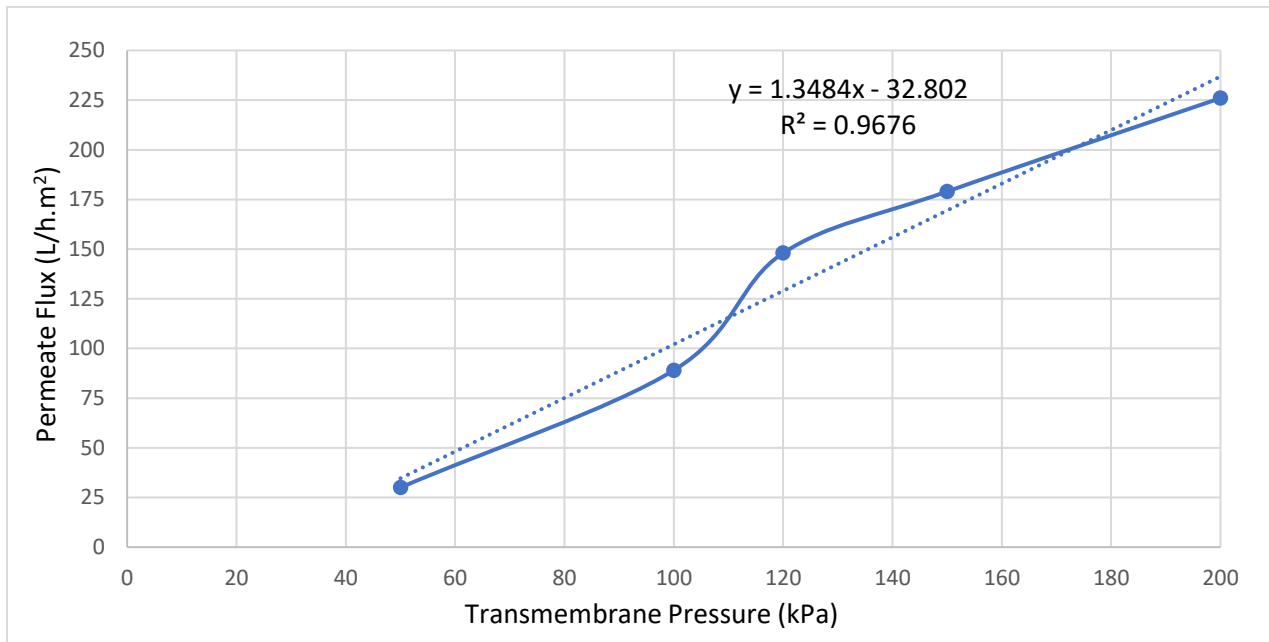


**Figure 4. 13 Effect of Transmembrane Pressure on Permeate Flux at pH 6,  $\text{NH}_4^+$ ,  $\text{NO}_3^-$ ,  $\text{PO}_4^{3-}$  = 100 mg/L, sophorolipid = 0.3%, TMP=120kPa, temperature=22°C and the sophorolipid concentration= 0.3%. The pH was 6, molecular weight cut-off (MWCO)=10,000, the flow rate = 70 rpm**

Furthermore, a linear connection between TMP and Flux shows negligible concentration polarization (Landaburu-Aguirre et al., 2010). The lowest flux was 30 L/h.m<sup>2</sup> at TMP=50 kPa, while the greatest flux was 226 L/h.m<sup>2</sup> at TMP= 200 kPa. Low transmembrane pressure reduces

operational expenses (Danis and Aydiner, 2009). Because its value was greater than the linear trendline in Figure 4.6, a first-order regression was determined as the best match.

#### 4.15 Effect of Transmembrane Pressure in Permeate Flux(Ions: SL=13.5:1)

As shown in Figure 4.14, increasing the transmembrane pressure (TMP) positively influences permeate flow, implying that as the TMP increases, the driving force starts to rise, resulting in higher flux. Furthermore, a linear relation between TMP and flux shows negligible concentration polarization (Landaburu-Aguirre et al., 2010).

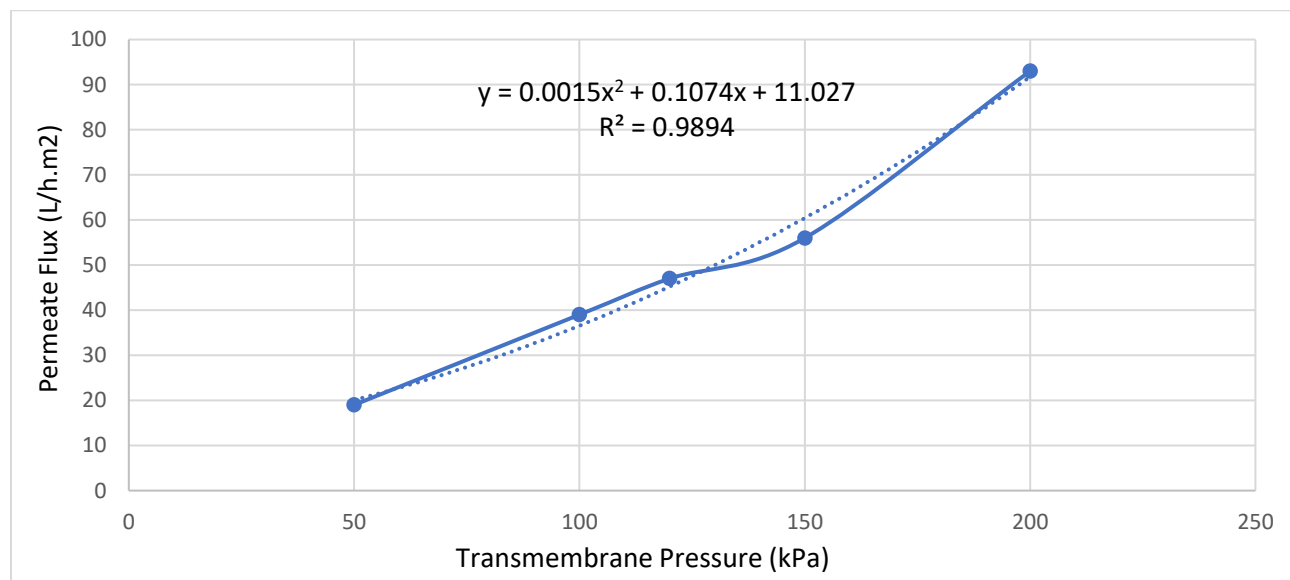


**Figure 4. 14 Effect of Transmembrane Pressure on Permeate Flux at pH 6,  $\text{NH}_4^+$ ,  $\text{NO}_3^-$ ,  $\text{PO}_4^{3-}$  =575, 2042 and 818.96 mg/L and sophorolipid = 0.03%, the pH was 6, molecular weight cut-off (MWCO)=10,000, the flow rate = 70 rpm**

The lowest flux was 19 L/h.m<sup>2</sup> at TMP=50 kPa, while the greatest flux was 93 L/h.m<sup>2</sup> at TMP= 200 kPa. The lowest transmembrane pressure is sought to reduce operational expenses

(Danis and Aydiner, 2009). Because the  $R^2$  value was high in Figure 4.13, first-order regression was the best match.

#### 4.16 Permeate flux Over Time (Ions: SL=1:1.3)

The influence of fouling on permeate flow was evaluated in this experiment at various periods (2, 5, 10, 15, and 20 minutes). At the same time, other parameters remained constant during the test. Fouling is a critical parameter in the performance of micellar-enhanced ultrafiltration, as shown in Figure 4.15.

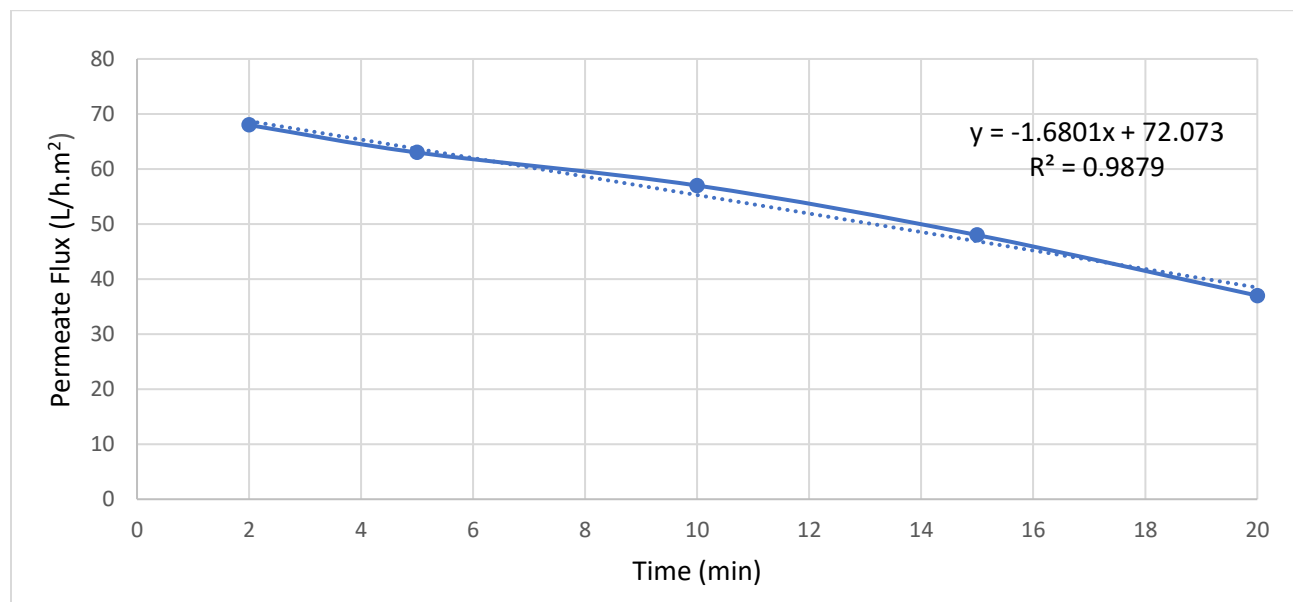


**Figure 4. 15 Effect permeate flux over time at pH 6,  $\text{NH}_4^+$ ,  $\text{NO}_3^-$ ,  $\text{PO}_4^{3-}$  = 100 mg/L and sophorolipid concentration = 0.3%, TMP=120 kPa**

#### 4.17 Permeate flux Over Time (Ions: SL=13.5:1)

The influence of time on permeate flux was evaluated in this experiment (2, 5, 10, 15, and 20 minutes). At the same time, other parameters, such as starting concentration, temperature,

pH, and transmembrane pressure, remained constant during the test. Fouling is a critical parameter in the performance of micellar-enhanced ultrafiltration, as shown in Figure 4.14. The equation is second-order, as represented by the equations in Figure 4.16.

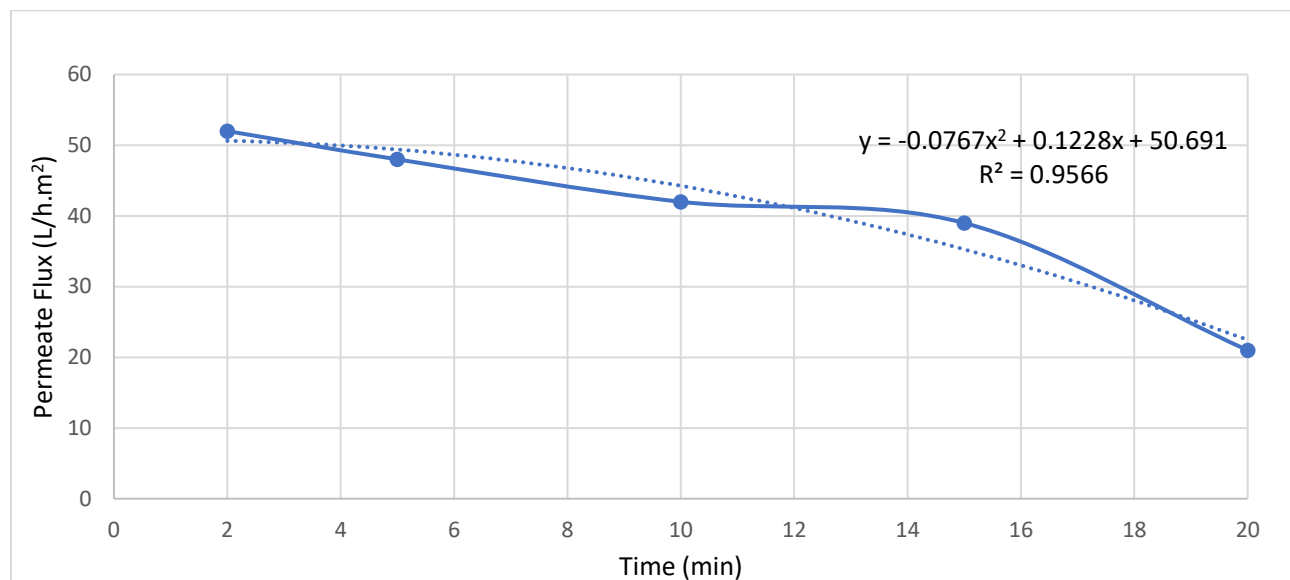


**Figure 4. 16 Effect of Permeate Flux over time at pH 6,  $\text{NH}_4^+$ ,  $\text{NO}_3^-$ ,  $\text{PO}_4^{3-}$  =575, 2042 and 818.96 mg/L and Sophorolipid = 0.03%**

The pollutant anions and cations were bound to the hydrophilic parts of the sophorolipid. The aggregates could not pass through the membrane because they were larger than the pore sizes of the hollow fiber membrane filter. Meanwhile, clean water with a smaller amount of sophorolipid and pollutant ions passes through the membrane. Fouling is generally a time-dependent and irreversible phenomenon (Ilias and Govind, 1993). With time, fouling is increased, and the fouling of the ultrafiltration membrane restricts the efficient production of drinking water (Yenphan et al., 2010).

## Chapter 5: Conclusions

The primary purpose of this research was to evaluate the efficiency of sophorolipid for removing ammonia, phosphate, and nitrate from water. For removing the ammonia, phosphate, and nitrate ( $\text{NH}_4^+$ ,  $\text{NO}_3^-$ ,  $\text{PO}_4^{3-}$ ) sophorolipid was used as a biosurfactant in this research's micellar enhanced ultrafiltration (MEUF) system. For the reduction of ammonia, phosphate, and sulphate, several factors such as pH, initial concentration of anions, sophorolipid concentration, temperature, and transmembrane pressure were examined to find the best condition for each factor. Sophorolipid has a significant role in removing ammonia, phosphate, and sulphate by the MEUF system when it is used at a concentration more than its critical micellar concentration. The ions ( $\text{NH}_4^+$ ,  $\text{NO}_3^-$ ,  $\text{PO}_4^{3-}$ ) were bound to the hydrophilic parts of the sophorolipid. The aggregates could not pass through the membrane because they were larger than the pore sizes of the hollow fiber membrane filter, while clean water with a very low amount of sophorolipid and ions ( $\text{NH}_4^+$ ,  $\text{NO}_3^-$ ,  $\text{PO}_4^{3-}$ ) were passing through the membrane. In this part of the research, the influence of some of the operating factors, such as transmembrane pressure (TMP), temperature, fouling, and sophorolipid concentration, on the performance of the MEUF system was investigated. Also, the behavior of sophorolipid in the presence of ions ( $\text{NH}_4^+$ ,  $\text{NO}_3^-$ ,  $\text{PO}_4^{3-}$ ) was observed. Based on the experimental results, the following conclusions were obtained from this work.

The parameters such as pH, initial concentration, and sophorolipid concentration had various effects on the percentage of anions and cation ( $\text{NH}_4^+$ ,  $\text{NO}_3^-$ ,  $\text{PO}_4^{3-}$ ) reduction percentage. The initial concentration of ions ( $\text{NH}_4^+$ ,  $\text{NO}_3^-$ ,  $\text{PO}_4^{3-}$ ) and pH decreasing and sophorolipid concentration by increasing had a significant effect on the reduction of  $\text{NO}_3^-$ ,  $\text{PO}_4^{3-}$ . Each sample had a pH of 6 and was produced at 100 mg/L for  $\text{NH}_4^+$ , 100 mg/L for  $\text{PO}_4^{3-}$ , and 100 mg/L for

$\text{NO}_3^-$ ; concentration of sophorolipid= 0.3% were selected as the best conditions for reduction of anions by sophorolipid. Temperature and transmembrane pressure as operating factors played essential roles in the micellar-enhanced ultrafiltration system process. By increasing both, the flux increased. However, the influence of transmembrane pressure was more than the effect of temperature on the flux. However, the concentration of sophorolipid in the permeate remained constant at all feed concentrations. Sophorolipid, as a biosurfactant in a micellar enhanced ultrafiltration system, was very effective for removing nutrients from the water.

The recommendations for future studies are to:

1. Evaluate the effect of sophorolipid on removing ions ( $\text{NH}_4^+$ ,  $\text{NO}_3^-$ ,  $\text{PO}_4^{3-}$ ) from actual contaminated water and wastewater.
2. Examine the influence of other biosurfactants and their mixture on removing ions ( $\text{NH}_4^+$ ,  $\text{NO}_3^-$ ,  $\text{PO}_4^{3-}$ ) with the MEUF system.
3. Determine the effect of other components such as Ca, Mg, Fe, and organic matter on removing ions ( $\text{NH}_4^+$ ,  $\text{NO}_3^-$ ,  $\text{PO}_4^{3-}$ ) by using the MEUF system.
4. Determine fouling mechanisms in removing ions ( $\text{NH}_4^+$ ,  $\text{NO}_3^-$ ,  $\text{PO}_4^{3-}$ ) by the MEUF system and investigate how to reduce it.

## References

- Abbasi-Garravand, E., & Mulligan, C. N. (2014). Using micellar enhanced ultrafiltration and reduction techniques for removal of Cr(VI) and Cr(III) from water. *Separation and Purification Technology*, 132, 505–512. <https://doi.org/10.1016/j.seppur.2014.06.010>
- Baek, K., Kim, B. K., Cho, H. J., & Yang, J. W. (2003). Removal characteristics of anionic metals by micellar-enhanced ultrafiltration. *Journal of Hazardous Materials*, 99(3), 303–311. [https://doi.org/10.1016/S0304-3894\(03\)00063-3](https://doi.org/10.1016/S0304-3894(03)00063-3)
- Batista, S. B., Mounteer, A. H., Amorim, F. R., & Tótola, M. R. (2006). Isolation and characterization of biosurfactant/bioemulsifier-producing bacteria from petroleum contaminated sites. *Bioresource Technology*, 97(6), 868–875. <https://doi.org/10.1016/j.biortech.2005.04.020>
- Camargo, J. A., & Alonso, Á. (2006). Ecological and toxicological effects of inorganic nitrogen pollution in aquatic ecosystems: A global assessment. *Environment International*, 32(6), 831–849. <https://doi.org/10.1016/j.envint.2006.05.002>
- Chen, M., Jafvert, C. T., Wu, Y., Cao, X., & Hankins, N. P. (2020). Inorganic anion removal using micellar enhanced ultrafiltration (MEUF), modeling anion distribution and suggested improvements of MEUF: A review. *Chemical Engineering Journal*, 398(January), 125413. <https://doi.org/10.1016/j.cej.2020.125413>
- Deriszadeh, A. (2009). *Improved MEUF Treatment of Produced Water Utilizing Naphthenic Acid Co-contaminants* IN PARTIAL FULFILLMENTS OF THE REQUIREMENTS FOR THE DEGREE OF DOCTORATE OF PHILOSOPHY FOR DEPARTMENT OF CHEMICAL AND PETROLEUM ENGINEERING). University of Calgary, Calgary, Alberta.

- El Zeftawy, M. A. M., & Mulligan, C. N. (2011). Use of rhamnolipid to remove heavy metals from wastewater by micellar-enhanced ultrafiltration (MEUF). *Separation and Purification Technology*, 77(1), 120–127. <https://doi.org/10.1016/j.seppur.2010.11.030>
- Ferraz, F. M., Povinelli, J., & Vieira, E. M. (2013). Ammonia removal from landfill leachate by air stripping and absorption. *Environmental Technology (United Kingdom)*, 34(15), 2317–2326. <https://doi.org/10.1080/09593330.2013.767283>
- Fu, H. Y., Zhang, Z. Bin, Chai, T., Huang, G. H., Yu, S. J., Liu, Z., & Gao, P. F. (2017). Study of the removal of aniline from wastewater via MEUF using mixed surfactants. *Water (Switzerland)*, 9(6). <https://doi.org/10.3390/w9060365>
- Fu, Q., Zheng, B., Zhao, X., Wang, L., & Liu, C. (2012). Ammonia pollution characteristics of centralized drinking water sources in China. *Journal of Environmental Sciences (China)*, 24(10), 1739–1743. [https://doi.org/10.1016/S1001-0742\(11\)61011-5](https://doi.org/10.1016/S1001-0742(11)61011-5)
- Ghadge, S., Chavan, M., Divekar, A., Vibhandik, A., Pawar, S., & Marathe, K. (2015). Mathematical Modelling for Removal of Mixture of Heavy Metal Ions from Waste-Water Using Micellar Enhanced Ultrafiltration (MEUF) Process. *Separation Science and Technology (Philadelphia)*, 50(3), 365–372. <https://doi.org/10.1080/01496395.2014.973515>
- Hilal, N., Al-Zoubi, H., Darwish, N. A., Mohammad, A. W., & Abu Arabi, M. (2004). A comprehensive review of nanofiltration membranes: Treatment, pretreatment, modelling, and atomic force microscopy. *Desalination*, 170(3), 281–308. <https://doi.org/10.1016/j.desal.2004.01.007>
- K.S.M., R., & E., G. (2008). Production, Characterisation and Applications of Biosurfactants-Review. *Biotechnology*, 7(2), 360–370. <http://tees.openrepository.com/tees/handle/10149/93896>

- Kang, G. dong, & Cao, Y. ming. (2012). Development of antifouling reverse osmosis membranes for water treatment: A review. *Water Research*, 46(3), 584–600.  
<https://doi.org/10.1016/j.watres.2011.11.041>
- Kim, B. K., Baek, K., & Yang, J. W. (2004). Simultaneous removal of nitrate and phosphate using cross-flow micellar-enhanced ultrafiltration (MEUF). *Water Science and Technology*, 50(6), 227–234. <https://doi.org/10.2166/wst.2004.0380>
- Kurniawan, T. A., Lo, W. H., & Chan, G. Y. S. (2006). Physico-chemical treatments for removal of recalcitrant contaminants from landfill leachate. *Journal of Hazardous Materials*, 129(1–3), 80–100. <https://doi.org/10.1016/j.jhazmat.2005.08.010>
- Ladewig, B., & Al-Shaeli, M. N. Z. (2017). *Fundamentals of Membrane Bioreactors* (Issue October). <https://doi.org/10.1007/978-981-10-2014-8>
- Liu, D. H., & Lipták, B. G. (1999). *Groundwater and surface water pollution* (1st edn). Lewis publishers, NY, USA.
- Liu, L., Luo, X. B., Ding, L., & Luo, S. L. (2018). Application of Nanotechnology in the Removal of Heavy Metal From Water. *Nanomaterials for the Removal of Pollutants and Resource Reutilization*, 83–147. <https://doi.org/10.1016/B978-0-12-814837-2.00004-4>
- Makkar, R. S., & Cameotra, S. S. (1999). Biosurfactant production by microorganisms on unconventional carbon sources. *Journal of Surfactants and Detergents*, 2(2), 237–241.  
<https://doi.org/10.1007/s11743-999-0078-3>
- Miao, L., Yang, G., Tao, T., & Peng, Y. (2019). Recent advances in nitrogen removal from landfill leachate using biological treatments – A review. *Journal of Environmental Management*, 235(November 2018), 178–185.  
<https://doi.org/10.1016/j.jenvman.2019.01.057>

- Moreno, M., Mazur, L. P., Weschenfelder, S. E., Regis, R. J., de Souza, R. A. F., Marinho, B. A., da Silva, A., de Souza, S. M. A. G. U., & de Souza, A. A. U. (2022). Water and wastewater treatment by micellar enhanced ultrafiltration – A critical review. *Journal of Water Process Engineering*, 46(January). <https://doi.org/10.1016/j.jwpe.2022.102574>
- Mulligan, C. N., Yong, R. N., & Gibbs, B. F. (2001). Surfactant-enhanced remediation of contaminated soil: A review. *Engineering Geology*, 60(1–4), 371–380. [https://doi.org/10.1016/S0013-7952\(00\)00117-4](https://doi.org/10.1016/S0013-7952(00)00117-4)
- Mulligan, C. N., & Sharifi-Nistanak, M. (2016). Conversion of sludge from a wastewater treatment plant to a fertilizer. *International Journal of GEOMATE*, 11(1), 2194–2199. <https://doi.org/10.21660/2016.23.1186>
- Mungray, A. A., Kulkarni, S. V., & Mungray, A. K. (2012). Removal of heavy metals from wastewater using micellar enhanced ultrafiltration technique: A review. *Central European Journal of Chemistry*, 10(1), 27–46. <https://doi.org/10.2478/s11532-011-0134-3>
- Namaghi, H. A., & Mousavi, S. M. (2014). Micellar-enhanced ultrafiltration of soft drink wastewater using anionic and mixed anionic/nonionic surfactants. *Journal of the Taiwan Institute of Chemical Engineers*, 45(4), 1850–1854. <https://doi.org/10.1016/j.jtice.2014.03.015>
- Papp, J.F. and B.R. Lipin, 2010. (n.d.). . *Kirk-othmer encyclopedia of chemical technology*. John Wiley & Sons, Inc., Accessed: May 2012, <http://onlinelibrary.wiley.com>.
- Peng, Z., Chen, H., Li, Y., Feng, K., Wang, C., Liao, F., Deng, H., & Huang, Y. (2020). Chelating surfactant for the removal of heavy metals from wastewater and surfactant recovery. *Desalination and Water Treatment*, 206, 229–234. <https://doi.org/10.5004/dwt.2020.26302>

- Puasa, S. W., Ruzitah, M. S., & Sharifah, a S. a K. (2011). An overview of Micellar - Enhanced Ultrafiltration in Wastewater Treatment Process. *International Conference on Environment and Industrial Innovation*, 12, 167–172.
- Rahmati, N. O., Pourafshari Chenar, M., & Azizi Namaghi, H. (2017). Removal of free active chlorine from synthetic wastewater by MEUF process using polyethersulfone/titania nanocomposite membrane. *Separation and Purification Technology*, 181, 213–222. <https://doi.org/10.1016/j.seppur.2017.03.030>
- Robert, M., Mercadé, M. E., Bosch, M. P., Parra, J. L., Espuny, M. J., Manresa, M. A., & Guinea, J. (1989). Effect of the carbon source on biosurfactant production by *Pseudomonas aeruginosa* 44T1. *Biotechnology Letters*, 11(12), 871–874. <https://doi.org/10.1007/BF01026843>
- Sadr, S. M. K., & Saroj, D. P. (2015). Membrane technologies for municipal wastewater treatment. In *Advances in Membrane Technologies for Water Treatment: Materials, Processes and Applications*. Elsevier Ltd. <https://doi.org/10.1016/B978-1-78242-121-4.00014-9>
- Samal, K., Das, C., & Mohanty, K. (2017). Application of saponin biosurfactant and its recovery in the MEUF process for removal of methyl violet from wastewater. *Journal of Environmental Management*, 203, 8–16. <https://doi.org/10.1016/j.jenvman.2017.07.073>
- Samper, E., Rodríguez, M., De la Rubia, M. A., & Prats, D. (2009). Removal of metal ions at low concentration by micellar-enhanced ultrafiltration (MEUF) using sodium dodecyl sulfate (SDS) and linear alkylbenzene sulfonate (LAS). *Separation and Purification Technology*, 65(3), 337–342. <https://doi.org/10.1016/j.seppur.2008.11.013>
- Schwarze, M. (2017). Micellar-enhanced ultrafiltration (MEUF)-state of the art. *Environmental*

*Science: Water Research and Technology*, 3(4), 598–624.

<https://doi.org/10.1039/c6ew00324a>

Shekhar, S., Sundaramanickam, A., & Balasubramanian, T. (2015). Biosurfactant producing microbes and their potential applications: A review. *Critical Reviews in Environmental Science and Technology*, 45(14), 1522–1554.

<https://doi.org/10.1080/10643389.2014.955631>

Silva, S. N. R. L., Farias, C. B. B., Rufino, R. D., Luna, J. M., & Sarubbo, L. A. (2010). Glycerol as substrate for the production of biosurfactant by *Pseudomonas aeruginosa* UCP0992. *Colloids and Surfaces B: Biointerfaces*, 79(1), 174–183.

<https://doi.org/10.1016/j.colsurfb.2010.03.050>

Uysal, A., & Celik, E. (2019). Removal of metals and recovery of released nutrients from municipal and industrial sludge using different biosurfactants. *Desalination and Water Treatment*, 172(October 2018), 37–45. <https://doi.org/10.5004/dwt.2019.24917>

Valeri, P., Morrone, L. A., Romanelli, L., Amico, M. C., & Piccinelli, D. (1992). Effetti Dei Farmaci Antiinfiammatori Non Steroidei (Nsaids) Sulle Contrazioni Evocate Nell'Ileo Di Cavia. *Ars Pharmaceutica*, 33(1-4 PART II), 545–551.

Verma, S. P., & Sarkar, B. (2018). Simultaneous removal of Cd (II) and p-cresol from wastewater by micellar-enhanced ultrafiltration using rhamnolipid: Flux decline, adsorption kinetics and isotherm studies. *Journal of Environmental Management*, 213, 217–235.

<https://doi.org/10.1016/j.jenvman.2018.02.069>

Vibhandik, A. D., & Marathe, K. V. (2014). Removal of Ni(II) ions from wastewater by micellar enhanced ultrafiltration using mixed surfactants. *Frontiers of Chemical Science and Engineering*, 8(1), 79–86. <https://doi.org/10.1007/s11705-014-1407-0>

- Wang, C., Tan, J., Harle, G., Gong, H., Xia, W., Zheng, T., Yang, D., Ge, Y., & Zhao, Y. (2019). Ammonia Formation over Pd/Rh Three-Way Catalysts during Lean-to-Rich Fluctuations: The Effect of the Catalyst Aging, Exhaust Temperature, Lambda, and Duration in Rich Conditions. *Environmental Science and Technology*, 53(21), 12621–12628.  
<https://doi.org/10.1021/acs.est.9b03893>
- Wang, Z., Ma, J., Tang, C. Y., Kimura, K., Wang, Q., & Han, X. (2014). Membrane cleaning in membrane bioreactors: A review. *Journal of Membrane Science*, 468, 276–307.  
<https://doi.org/10.1016/j.memsci.2014.05.060>
- Yaqub, M., & Lee, S. H. (2019). Heavy metals removal from aqueous solution through micellar enhanced ultrafiltration: A review. *Environmental Engineering Research*, 24(3), 363–375.  
<https://doi.org/10.4491/EER.2018.249>
- Yenphan, P., Chanachai, A., & Jiratananon, R. (2010). Experimental study on micellar-enhanced ultrafiltration (MEUF) of aqueous solution and wastewater containing lead ion with mixed surfactants. *Desalination*, 253(1–3), 30–37.  
<https://doi.org/10.1016/j.desal.2009.11.040>
- Zeftawy El, M, M. A. (2007). *Use of rhamnolipid to remove heavy metals from aqueous streams via micellar enhanced ultrafiltration*. ( IN PARTIAL FULFILLMENTS OF THE REQUIREMENTS FOR THE DEGREE OF DOCTOR OF PHILISOPHY FOR DEPARTMENT OF BUILDING, CIVIL AND ENVIRONMENTAL ENGINEERING). Concordia University, Montreal.
- Zhao, Y., Ren, Y., Wang, X., Xiao, P., Tian, E., Wang, X., & Li, J. (2016). An initial study of EDTA complex based draw solutes in forward osmosis process. *Desalination*, 378(December 2017), 28–36. <https://doi.org/10.1016/j.desal.2015.09.006>

